ESD-TR-69-69

Technical Note

1969-24

R. T. Lacoss

A Large-Population LASA Discrimination Experiment

8 April 1969

Prepared for the Advanced Research Projects Agency
under Electronic Systems Division Contract AF 19(628)-5167 by

Lincoln Laboratory

MASSACHUSETTS INSTITUTE OF TECHNOLOGY

Lexington, Massachusetts

The work reported in this document was performed at Lincoln Laboratory, a center for research operated by Massachusetts Institute of Technology. This research is a part of Project Vela Uniform, which is sponsored by the U.S. Advanced Research Projects Agency of the Department of Defense; it is supported by ARPA under Air Force Contract AF 19(628)-5167 (ARPA Order 512).

MASSACHUSETTS INSTITUTE OF TECHNOLOGY
LINCOLN LABORATORY

A LARGE-POPULATION LASA DISCRIMINATION EXPERIMENT

R. T. LACOSS

Group 64

TECHNICAL NOTE 1969-24

8 APRIL 1969

LEXINGTON MASSACHUSETTS

ABSTRACT

A computer program has been written and has been applied to LASA time series data from nearly 200 events in order to obtain data for discrimination studies. In general the previously estimated performance of M_s-m_b, spectral ratio, and complexity has been corroborated. Some of the specific results are the following. Except for one anomalous earthquake, all shallow earthquakes with $m_b \rangle 4.8$ and explosions with $m_b \rangle 5.1$ have been correctly identified using M_s-m_b. No events with $m_b \langle 5.1$ could be unequivocally identified as explosions. However, the probability that an earthquake would be identified as such decreased to zero only gradually as m_b was reduced to about 4.0. A modification of spectral ratio has been made which introduced the option to make no decision concerning the nature of an event when the signal-to-noise ratio is not sufficiently large. The probability that no decision will be made is zero for $m_b \rangle 4.8$ and unity for $m_b \langle 4.0$. The probability of correct identification is high for events which pass the signal-to-noise ratio test. The period of short period P-waves may be a valuable discriminant at low magnitudes. Many earthquakes with magnitudes below 4.5 can be identified as such using the period data. Depth phase picks have been made for about 60% of the earthquakes in our population. About 70% to 95% of these picks correspond to valid depth phases. Unfortunately, depth phases were also picked for three presumed explosions.

Accepted for the Air Force
Franklin C. Hudson
Chief, Lincoln Laboratory Office

I. INTRODUCTION

Short-period data from the Large Aperture Seismic Array (LASA) has been used in the past to develop and evaluate single station seismic discriminants for events at teleseismic distances from the array. In 1966, Kelly[1] reported preliminary LASA results using complexity[2] as a discriminant. Later, in 1967, Briscoe and Walsh[3] reported initial success using a discriminant involving the frequency distribution of short-period energy (spectral ratio). More recently, Kelly[4] has evaluated these short-period discriminants using more extensive data.

The long-period data from LASA has been used in conjunction with the short period data to evaluate the ability of a single station to identify events based upon the relative excitation of body phases and surface phases.[5,6] (This is the so-called $M_s - m_b$ criteria.) Identification based on the $M_s - m_b$ criteria, but using many teleseismic stations, had been previously reported by Liebermann and Pomeroy.[7,8] Earlier results relating to the relative excitation of body and surface waves used only nearby stations.[9]

The Seismic Discrimination Group at Lincoln Laboratory has continued to investigate the discriminants considered by Kelly[4] and Capon, et al.[5,6] The present report is devoted primarily to further studies of single station discriminants which have been measured for a large population of almost 200 events.

It is noteworthy that the Lincoln Laboratory event processing procedures have now been considerably modified and standardized. This has greatly reduced the human effort required to obtain standard discriminants for individual events and has resulted in the generation of a library of events which can conveniently be used to aid in understanding standard discriminants or in discovering new ones. (The details of the new

event processing procedures can be found in Section III.) All processing of LASA waveforms for this report has been accomplished using a single computer program (SPLP) designed to completely process an event (both short-period and long-period data) during a single pass on a large digital computer.

The event population discussed in this report has been designed to at least partially rectify some of the deficiencies of the populations used previously. Previous populations, particularly for spectral ratio, included many large explosions and very few equally large earthquakes. The Lincoln Library of seismic data has been searched for large earthquakes which can be compared with the large explosions. The population of presumed explosions has been increased nearly 100% above that used by Kelly.[4]

Whenever possible, both long-period and short-period waveforms are now processed for each event. Thus this data can be considered jointly without great difficulty. The long-period and short-period data used in earlier reports[4,5,6] was obtained somewhat independently making it difficult to obtain a common data base. In addition, the procedures for data reduction which are now in use are uniformly applied to all events. Thus nuisance effects due to minor variations in the treatment of individual events have been minimized if not eliminated.

All measured diagnostics as well as short-period LASA beams and other data for all events in our population are stored on a single composite digital magnetic tape. New events can be added as desired. This digital tape storage of data has greatly aided in the study of standard discriminants. In addition, the data on the composite tape is currently being used to investigate possible multivariate use of the data from a single site.

The same program (SPLP) which has been used to generate the composite tape of LASA data can be applied to the short-period data currently being recorded at NORSAR. Thus a composite tape of data recorded in Norway can be generated. This is currently in progress for that subset of events in our data base which might have been sensed in Norway and for which recordings were made. Ultimately it is hoped that the LASA and NORSAR composite tapes can be used for a joint discrimination experiment in which data processing at both sites is as uniform as is feasible.

II. DATA BASE

The earthquake population considered in this report consists primarily of events believed to be in or very close to the Sino-Soviet bloc countries. In addition, the population includes four earthquakes in North Africa (Algeria, Tunisia), 10 earthquakes in the Mediterranean and Aegean Sea area, six earthquakes in the area of Iran, Iraq and western Turkey, and six earthquakes from the Laptev Sea and Arctic Ocean. Altogether the earthquake population consists of 156 events. Of these about 40% are in the Kurile-Kamchatka area.

The population of 35 presumed underground nuclear explosions includes events from Sahara and Amchitka (Longshot) in addition to events from Soviet test sites.

Our earthquake population is not representative of the natural seismicity of the earth. For example, LASA station bulletins were initially searched starting 1 January 1968 for events in or near the Sino-Soviet bloc countries. This population began to be biased towards events with magnitudes from 4.0 to 5.0 on the Richter scale and towards events from the Kurile-Kamchatka area. Events were then added only if they were large or from outside the Kurile-Kamchatka area. It was felt that the population was still deficient in large magnitude events so the entire Lincoln Laboratory tape library was searched for large events in the Sino-Soviet area which could be added. Some of these large earthquakes, as well as many of the nuclear explosions, were part of the data base for the experiments previously reported by Kelly[4] and by Capon, et al.[5] Figure 1 shows a cumulative histogram of the magnitude of the earthquake population. A line with the same slope as the natural seismicity curve has been drawn on the figure to emphasize that our population is not representative of natural seismicity.

Only about 55% of the earthquakes and about 70% of the presumed underground explosions included in our data have been reported by the U. S. Coast and Geodetic Survey (USCGS). This does not imply anything about the relative detection levels of LASA and USCGS. It does define the size of the population which we have used most extensively for checking the ability of a single large array to determine depth.

Our population of events includes many which are anomalous in one or more aspects. For example, consider Fig. 2 which is a plot of the LASA body-wave magnitudes against the USCGS magnitudes for both earthquakes and explosions. Events more than 99^{o} from LASA or with USCGS depths greater than 100 km have not been shown. There is general agreement between the two magnitudes with LASA tending to be slightly higher. The scatter of the main body of data is generally less than ± 0.5 magnitude units. A few points do scatter to magnitude discrepancies as large as 1.0 magnitude units. This data is included here to underline the fact that even using a large array to measure an event property as basic as magnitude will result in some scatter and occasionally very anomalous measurements. No attempt has been made to exclude events from our data base because of some anomalous behavior or properties. Individual events are discussed in other sections only when their anomalous behavior relates to discrimination. Thus an event with a large LASA-USCGS magnitude discrepancy would not be specifically discussed unless the discrepancy resulted in discrimination difficulties.

III. ROUTINE EVENT PROCESSING

Short-period and/or long-period seismograms for all events in our data base are recorded on standard format LASA digital tapes. As mentioned in Section I, a single computer program (Short-Period Long-Period or SPLP) has been written which normally allows us to complete all routine analyses of LASA data for an event in a single computer run with the LASA digital tapes for the event. In this Section we describe the operational characteristics of this program and the interaction of an analyst with the program.

SPLP will accept either Lo-Rate or Hi-Rate tape from LASA as input. If Lo-Rate tape is supplied, then both long-period and short-period analysis is done. The short-period data in this case are the 21 straight sum traces recorded on the tape. If Hi-Rate tape is supplied, the program operates with the twenty-one 500-ft seismometers at the center of each subarray and processes only short-period data. The program requires about 20 minutes of IBM 360/67 time to completely process an event. This is reduced to 10 – 15 minutes if only short-period data are available. It is likely that by restructuring and rewriting the program the processing time could be reduced. An absolute limitation to time reduction is imposed by the approximately eight minutes required to read through a complete input tape. SPLP also accepts the short-period data generated by the limited array in the area of Oyer, Norway.

Figure 3 is a flow chart indicating all of the major operations done by SPLP. Except for the entry of seismograms into core, no input or output has been shown. All measured or computed event parameters as well as beam waveforms and spectral curves are output graphically using an SC 4020 hard copy display and are also stored on a composite digital magnetic tape. Although many options are available, only a

small number of input parameters is changed for the routine processing of events. In particular, the program requires as an input rough estimates of P arrival time, azimuth, and horizontal phase velocity for the event. Arrival times within 20 seconds are quite sufficient, and the estimated azimuth (β) and horizontal phase velocity (v) supplied to the program can be quite crude. The arrival times, β, and v obtained from LASA station bulletins have proved to be more than sufficiently accurate. If the quality of β and v are thought to be particularly poor, a larger grid of SP beams can be requested.

The program can be requested to use any combination of long-period and short-period instruments to perform an analysis. Thus, for example, when it is known that a particular instrument is not operational, the program is requested to omit it from consideration. However, the program was designed to operate without the need to visually check every waveform to be used. Some simple checks are included to detect and reject bad data. The peak value and average absolute value for each channel of data are computed over the time interval of interest. Any channel for which either the peak or the average differs by more than a factor of five from the median channel is removed from consideration. This procedure has been quite successful in removing anomalous channels. More sophisticated tests of data, with possible data correction for isolated glitches in the waveform, might have saved a few of the channels rejected by the program and eliminated the cases in which intervention by an analyst was required to select satisfactory channels.

Bandpass filtering of all long-period and short-period data has been accomplished in the frequency domain as described in Appendix A. The 0.6 – 2.0 Hz and 0.025 – 0.055 Hz passbands indicated on Fig. 3 have been used for all events.

These passbands evolved from earlier experience with LASA data and test runs with SPLP. The bands can be changed by data cards submitted with SPLP. This is convenient since for example initial experience with Norway data indicates that a 0.6 – 3.5 Hz passband yields much more satisfactory operation than does 0.6 – 2.0 Hz, which often seriously degrades the signal. One might adjust the passband for each event but that would require significant pre-run analysis of the event.

Let v_{ON} and v_{OE} be the north and east components of velocity corresponding to the β and v input to SPLP for an event. The program forms a filtered short-period beam for an event with horizontal phase velocity components, v_{ON} and v_{OE}. LASA station corrections are added to the plane wave moveouts when forming the beam. A number of similar beams are formed about this central beam. Beams are formed, including station corrections, with velocity components

$$v_N = f_o \frac{k_{ON} + m\Delta k}{(k_{ON} + m\Delta k)^2 + (k_{OE} + n\Delta k)^2}$$

and

$$v_E = f_o \frac{k_{OE} + n\Delta k}{(k_{ON} + m\Delta k)^2 + (k_{OE} + n\Delta k)^2}$$

where f_o is a nominal event frequency read into the program, Δk is a wavenumber increment read into the program, n and m are positive or negative integers with limits read into the program,

$$k_{ON} = \frac{f_o v_{ON}}{v_{ON}^2 + v_{OE}^2} ,$$

and

$$k_{OE} = \frac{f_o \, v_{OE}}{v_{ON}^2 + v_{OE}^2} \quad .$$

The grid of beams formed is uniform in wavenumber. It is not uniform in location or velocity. The density of beams in wavenumber is fixed by Δk which is an input parameter. Most runs with LASA data have been made with $\Delta k = 0.00125$ c/km. The LASA 3 db beam width is about 0.005 c/km. Thus several beams will be formed within the main LASA beam. If an event is 85^o distant from LASA, the choice $\Delta k = 0.00125$ results in beams separated by roughly 2^o on the earth's surface. This is typical of the separation between beams.

Event location is done by choosing that filtered beam with the largest peak to peak excursion. Zero depth is assumed and the velocity for that beam is converted to bearing and distance from LASA. The resulting epicenter is not the best obtainable using LASA. The grid density and location procedure have been chosen to yield a location sufficient for our discrimination studies not to yield a best epicenter. Our current objective has not been to investigate discrimination based upon accurate epicenter determination.

The program uses the best filtered beam to estimate body-wave magnitude. The largest peak-to-peak excursion in the waveform and its period are measured. From this and distance the LASA magnitude is computed.[10]

Complexity is measured by SPLP using the best filtered beam. The definition of complexity used is

$$C = \int_5^{35} |x(t)| \, dt \; / \; \int_0^5 |x(t)| \, dt$$

where x(t) is the beam, the origin of time is at the event onset, and in practice the integrals are actually sums over data samples. The program has no algorithm for determining onset time. Only the time of the peak excursion of the beam is known. Thus the program computes several complexity values assuming various times from onset to peak value. An analyst has ultimate responsibility, guided by SC 4020 plots with time intervals indicated, for choosing which is the correct measurement. In some cases, for example a very emergent event, no complexity values are valid. If this is the case, the correct value is computed during a final many event editing run of the SPLP composite tape. The output tape from this editing run is described at the end of this Section and in Appendix B.

A very preliminary check for possible depth phases is done by SPLP. A short section of beam, typically five seconds, around the peak time is zeroed out. The remaining waveform is scanned to find the location of the largest peak which is greater than 0.25 of the peak in the blanked out interval. Such a peak is indicated on the SC 4020 output. Whenever possible, USCGS data is obtained for each event. If this data indicates a possible depth phase outside of the 102.8 second short-period window used by SPLP a second run is undertaken explicitly to detect any possible depth pulse. Ultimate responsibility for all phase picking is given to the analyst. His decisions about possible depth phases, if he is at variance with the program pick, are included during the final editing run.

The epicenter determined from filtered data is used to form an unfiltered short period beam waveform. This beam waveform is used to obtain spectra and to measure spectral ratio. Spectra have been computed for 10 and 20 second intervals including the event. The spectra are computed by discrete Fourier transforming the entire beam,

normally 102.8 seconds long, with all data outside the 10 or 20 second interval set to zero. The data is tapered linearly to zero over 1.0 seconds at the ends of the intervals. Just as is the case for complexity the onset time is not known. Thus several shifted intervals were used and the analyst picked the appropriate one. If none were satisfactory, this was corrected during the final composite tape editing run.

Spectral ratio is computed for both the 10 second and 20 second intervals. The definition has been changed from that used previously by Briscoe[3] and Kelly.[4] Specifically, SPLP computes

$$R = \int_{1.45}^{1.95} |X(f)|\, df \Big/ \int_{0.35}^{0.85} |X(f)|\, df$$

where $|X(f)|$ is the magnitude of the 10 or 20 second interval spectra and in practice the integrals are replaced with sums over frequency components.

Travel time tables for Rayleigh as well as P waves are included in SPLP. Thus once all the short-period data is processed, it automatically moves to the appropriate time interval and begins processing long-period data.

Beamforming of long-period data is done with no station corrections and no correction for the slightly different velocities of the different frequency components of the long-period events. Both of these refinements would result in at best a trivial improvement of the beams. The nominal Rayleigh wave velocity used for steering has been determined by measuring events. The surface waves are assumed to arrive from the same azimuth as the P waves.

Unlike earlier experiments[5] all chirp filtering is done in the frequency domain as is described in Appendix A. Chirp filters with impulse response durations ranging

from 200 seconds to 800 seconds in increments of 50 seconds are applied to the vertical long-period beam. Matched filtering such as that used by Alexander[11] has not been used. The chirp filtered beam with the largest zero to peak excursion is saved to compute a number which should differ from surface wave magnitude by only an additive constant.

Specifically, SPLP computes

$$L = \log_{10} A + 1.66 \log_{10} \Delta$$

where A is the amplitude of the largest chirp waveform and Δ is epicentral distance. The relation of L to M_s, the surface wave magnitude,[12] is discussed in Section IV.

The analyst, utilizing plots of all long-period beams including chirp filtered radial and vertical beams, has the ultimate judgments to make about the long-period data. He must decide if (1) the program has picked the event properly, (2) no signal is actually visible above the background noise, or (3) some other event has arrived at about the same time and obscured the event of interest.

Much of the data recorded on the SPLP composite tape is redundant, unwanted, obsoleted by later data on the same tape, or should be modified or corrected by inputs from an analyst. This is done simultaneously for all events on the composite tape using edit programs designed for the purpose. The output of the edit program is an 800 bpi 9-track tape with a single logical record for each successfully processed event on the SPLP composite tape. Each logical record is written by an IBM 360 Fortran IV write statement. The record format is specified as variable with a blocksize of 2688 bytes and a record length of 2684 bytes. It is this tape which we have used for our discrimination studies. Appendix B shows the structure of each logical record. Copies of this edited tape are available to qualified requesters of LASA data.

IV. CALIBRATION FOR SURFACE WAVE MAGNITUDE

The SPLP program does not directly generate a surface wave magnitude. It does generate a surface wave factor, L, which was defined in Section III. For Δ between 15^{o} and 130^{o} Gutenberg[12] gives surface wave magnitude as

$$M_s = \log_{10} A' + 1.66 \log_{10} \Delta + 1.82$$

where A' is the horizontal component of the maximum ground movement in microns during surface waves having periods of about 20 seconds. This expression for M_s ignores station effects and the depth of events. The surface factor and surface wave magnitude are approximately related by

$$M_s = L + 1.7$$

This relation was determined by the calibration procedures described below and has been used throughout this report to obtain M_s values for events.

One approach is to assume that the horizontal and vertical components of the LP Rayleigh wavetrain will have approximately the same amplitude. Assume also that the peak of the best chirp filtered wavetrain is B times the peak of the input wavetrain. That is, we assume that BA' = A, where A is the amplitude of the chirp output. It then follows that

$$M_s = L + 1.82 - \log_{10} B$$

We have measured B for a collection of 33 earthquakes and 10 bombs which had clear surface waves before chirp filtering. The value of B obtained for earthquakes was

1.48 and for the explosions, 1.68. The overall average value of B was thus 1.53. Using this value of B gives $M_s = L + 1.63$.

Another calibration approach has been to compare L with M_s values independently reported for the same events. This has been done for 10 earthquakes and seven explosions in our data base which have had surface wave magnitudes independently measured. The events for comparison had M_s determined previously using either unprocessed seismograms or time-domain chirp filtering methods.[5,6] This comparison gave $M_s = L + 1.72$.

The relationship $M_s = L + 1.7$ has been accepted as a reasonable compromise between those obtained by the above calibration procedures.

Figure 4 is a plot of $M_s = L + 1.7$ versus LASA body-wave magnitude for earthquakes in our population. The plot includes a number of events never reported by USCGS, but all events located deeper than 100 km by USCGS have been excluded. The empirical relationship $M_s = 1.59\, m_b - 3.97$, determined by Gutenberg and Richter[10] has been drawn on the figure. This line is a reasonable average line for the data shown. This plot, which is in fact a somewhat different method of calibration, verifies the validity of the relationship of M_s and L.

V. SURFACE WAVE DETECTION PROBABILITY

Capon, et al,[5] have previously considered the same geographical area as we are considering and reported that surface waves were detected by LASA for all earthquakes with body-wave magnitudes greater than about 4.9. Our data has substantiated those results by achieving a 100% detection threshold of 4.8. In addition, we have considered our data in sufficient detail to obtain estimates of the probability of detection of surface waves for each value of body-wave magnitude.

Figure 5 shows three incremental histograms for three sets of events in our population. The top is for all earthquakes for which we detected surface waves. The bottom plot is for all earthquakes which had surface waves obscured by the simultaneous arrival of surface wave trains from comparable or larger events. The center plot is for earthquakes with surface waves obscured by the continuous background seismic noise. The magnitude boxes used to construct these histograms were each 0.1 body-wave magnitude unit wide. No histogram is shown of the events for which equipment or tape problems precluded the detection of surface waves.

Figure 6 was constructed from the upper two histograms on Fig. 5. The dots represent the incremental detection probability computed by taking the ratio of detected events to total events in each magnitude range. Events deeper than 100 km were excluded in constructing Fig. 6. The scatter of the data is large. The 100% detection at $m_b = 4.8$ is probably optimistic although it appears reasonable to accept a value as large as 90%.

The detection probability can be estimated in a different way using measured noise properties. The approach is much more indirect. Nevertheless, the results are not inconsistent with the direct estimates.

Indirect estimates were obtained as follows. First, all events with no detected surface waves were used to construct Fig. 7. The figure was constructed by using the largest noise burst and the distance to the event to compute M_s values. Although the resulting distribution of M_s values may be biased high, Fig. 7 is interpreted to be the distribution of detectable surface wave magnitudes if detection is always possible at 0.0 db signal-to-noise ratio. Thus for example, if detection is always possible at 0.0 db, then approximately 50% of all events with surface wave magnitude 2.9 will be detected since the noise will be less than that equivalent M_s value 50% of the time. If a different SNR is required for detection, then the curve of Fig. 7 must be shifted to obtain the probability of detection for a given M_s value. For example, if 3 db of SNR is required, the curve must be moved to the right by 3/20 surface-wave magnitude units. In this case the detection probability for events with $M_s = 2.9$ is reduced from 0.5 to about 0.25. Once the SNR required for detection is established it is now easy to obtain the probability of detection of surface waves as a function of m_b rather than M_s. Figure 8 shows such curves for 3.0 db and 6.0 db SNR required for detection. Those curves are simply generated from the appropriately shifted curves of Fig. 7 by assuming the Gutenberg-Richter relationship $M_s = 1.59\, m_b - 3.97$.[10]

There is fair agreement between the detection probabilities shown in Fig. 8 (3 db curve) and in Fig. 6. Both curves indicate that the incremental detection probability for earthquakes is 0.5 for m_b about equal to 4.5 and increases to nearly 1.0 at $m_b = 4.8$. The 3.0 db SNR required for detection is not unreasonable for an analyst who can make use of time windows and his ability to recognize waveform characteristics.

The preceding discussion of detection probabilities did not consider events obscured by interfering events. It is clear from Fig. 5 that interference can be a

nontrivial problem. However, since our data is not particularly representative of natural seismicity, we have not attempted to consider the problem in great detail. Our data simply sets the order of magnitude of the problem.

VI. $M_s - m_b$ DISCRIMINATION

The relative excitation of surface waves and body waves by earthquakes and underground explosions has previously been established as a powerful discriminant. The data presented in this Section essentially corroborates the usefulness of the $M_s - m_b$ discriminant.

Figure 9 shows a scatter diagram of M_s vs m_b for 69 earthquakes with detected surface waves and 10 presumed explosions with detected surface waves. Both M_s and m_b are the values measured using SPLP. There is a good separation of the two populations except for a few earthquakes which appear to have low surface-wave magnitudes. Figure 10 shows the scatter diagram after removing the five events in the population of Fig. 9 which were reported at depths greater than 100 km by USCGS. In addition, M_s upper bounds for five presumed explosions with surface waves obscured by noise have been shown on the plot. The separation between bombs and earthquakes is now clearly better. A comparison of the two figures shows that all events removed by the depth filter had relatively small surface waves resulting in small values of M_s. This is to be expected since deep events should be less efficient producers of surface waves than events at normal depths.

One earthquake remains entirely within the explosion region of Fig. 10. That event is located just west of the Kurile Islands. The P-wave arrival at LASA was at 16:14:50 on 23 December 1967. It has been reported and located by USCGS as well as by LASA. The event is in fact not a real discrimination problem since it is located well off of any land by USCGS and there is a clear arrival at LASA which, if it is assumed to be pP, locates the event at about 33 km depth. The depth is corroborated by the 26 km unrestrained depth obtained by USCGS. In addition, the first motion recorded at LASA

is clearly dilatational (Event E on Fig. 26.) Despite all of this the event is a problem since such a shallow event should more effectively generate surface waves.

The USCGS has assigned a body-wave magnitude of 5.1 to the problem event whereas LASA has assigned it 5.7. Since the USCGS m_b would make the event more like an earthquake it was decided to plot the LASA M_s against the USCGS m_b for all events on Fig. 10 which were also reported by USCGS. Figure 11 is that plot. Although the problem event still has an unusually low value of M_s the separation between earthquakes and explosions is now complete. It should probably be noted that the $m_b = 5.0$ explosion had marginally detected Rayleigh waves. The measured M_s for that event may be slightly high due to noise.

A comparison of Figs. 10 and 11 suggests that the m_b values obtained from a worldwide system (USCGS in this case) is more stable and effective for discrimination than that obtained from a single large array station. Various arguments revolving around P-wave radiation patterns can be employed to substantiate such claims. The experimental data at hand is certainly not conclusive. For example, since USCGS did not report all events in our population, Fig. 11 contains many fewer points than Fig. 10.

The value of M_s measured at a site is also a function of the radiation pattern of the event. This might also be affecting the discrimination ability of LASA based upon $M_s - m_b$.

It is generally believed[5,6] that the $M_s - m_b$ criteria should be regionalized. That is, only explosions and earthquakes from the same tectonic region should be compared. This is not contradicted by our data but neither is it very strongly substantiated. For example, the percentages of normal depth events above and below the line $M_s = 1.59\, m_b - 3.97$ have been computed. Using the LASA m_b gives 57% below the line for

Kurile-Kamchatka earthquakes and only 33% for the remaining earthquakes in our population. If the USCGS m_b is used, the figures become 44% and 30%, respectively. This tends to substantiate the assertion that events from the Kurile-Kamchatka area often have small surface waves. The strongest support for regionalization in our data may be the 23 December 1967 problem event which is from the Kurile Islands region. None of the presumed explosions with detected surface waves are from that region.

It appears that the M_s-m_b criterion can be successfully applied to most earthquakes with $m_b > 4.8$ since M_s can be measured for such events. As m_b is reduced to about 4.0, the probability of identification is reduced to zero as the probability of surface wave detection goes to zero. All presumed explosions in our data base with $m_b > 5.1$, exclusive of those subjected to interfering events or with no tape available, have been correctly identified using M_s-m_b. It has not been possible to apply M_s-m_b to any of the smaller presumed explosions. It would thus appear that many earthquakes can be identified as such using M_s-m_b at lower body wave magnitudes than those at which explosions can be identified using M_s-m_b.

VII. BASIC SPECTRAL RATIO DISCRIMINATION

As mentioned in Section III spectral ratio has been calculated using a 10-second interval and a 20-second interval of data for each event. The two spectral ratios were approximately equal in most cases. In general, we have found no significantly better discrimination using one rather than the other of these two spectral ratios. Since the 10-second measure will tend to have a slight signal-to-noise advantage and will less often include clear depth phases in the interval we have tended to use it rather than the 20-second measure. In the remainder of this section only the 10-second spectral ratio is considered. A comparison of 10 and 20 second results is given in Section VIII after events have been removed from the population by virtue of unsatisfactory signal-to-noise ratios.

Figure 12 is a scatter diagram of spectral ratio vs the LASA m_b for all underground explosions and all earthquakes with distances less than 99^o. The decision line shown on the figure is an exponential and is the geometrical mean of the two indicated population trends. None of these lines has been formally optimized but were obtained as described in the following paragraph.

The spectral ratio of an event is the ratio of two quantities derived from the spectrum of the event. Let V_H and V_L be these quantities obtained from the 1.45 – 1.95 Hz (high) band and the 0.35 – 0.85 Hz (low) band, respectively. Figures 13 and 14 show V_H and V_L scattered against LASA m_b on semilog paper. These figures were used to obtain the decision lines and trend lines shown on Fig. 12. The trends of the data on Figs. 13 and 14 appear to be well represented by straight lines. The straight lines drawn on the figures were selected visually to obtain a good fit to the data. A nominal spectral ratio as a function of magnitude was obtained for each type of event by

using the appropriate trend lines on Figs. 13 and 14. These nominal spectral ratios are the trend lines shown on Fig. 12. Note that spectral ratio discrimination is equivalent to using $\log V_H - \log V_L$ as a discriminant. The decision line shown on Fig. 12 is equivalent to using the arithmetic means of the log of spectral ratio trends as a decision line and the log of spectral ratio as a discriminant.

Figure 15 shows a plot of spectral ratio vs LASA m_b for the same events as Fig. 12 except for those events located deeper than 100 km by USCGS. Several of the earthquakes on the explosion side of the decision line on Fig. 12 were deep and do not appear on Fig. 15. This is quite reasonable since P waves from deep events travel through less low Q material to reach the receiving station. It may also be possible that the deep events actually generate more high frequency signals than do normal depth events. In any case it is clear that spectral ratio does not operate well for deep events. Somehow deep events must be identified as such and excluded from further consideration. This is consistent with earlier results.[4]

In Section VI it was suggested that $M_s - m_b$ discrimination might be improved by the use of USCGS m_b rather than LASA m_b. Our study of the data has not unearthed any such preference in the case of spectral ratio. Either the LASA or the USCGS m_b seem to be equally effective for discrimination.

In addition to the deep events, there are still others which should be excluded from spectral ratio tests. These are events for which the spectral ratio is too extremely distorted by the background noise to be meaningful. This problem is considered in Section VIII. It will be shown in particular that the two presumed explosions incorrectly classified on Fig. 15 should be discounted since the SNR is too low for those events.

VIII. MODIFIED SPECTRAL RATIO DISCRIMINATION

The spectral ratio measured for any event is in fact a measure for the sum of signal and background noise. Ideally there would be no background noise. This condition is essentially obtained for very large events. However, it is clear that the measured spectral ratio must be increasingly affected by noise as events get smaller. In the limit the measured spectral ratio is a measure of noise properties and has nothing at all to do with the signal. This signal-to-noise ratio problem has been previously noted by Kelly.[4] He estimated that spectral ratio could be reliably applied to events with $m_b \geq 4.5$. The effects of noise contamination have now been studied in greater detail and results described below. One fact which has become apparent is that the validity of individual measurements can be determined by considering the noise preceding the event.

The short-period beams for all events are recorded on the composite event tape. In most cases about 30 seconds of data is included preceding the event arrival. It has thus been possible to obtain two 10-second noise intervals immediately preceding each event as well as a 10-second interval containing the event. The intervals do not overlap. These three intervals have been used to study the effect of noise upon spectral ratio.

Recall that V_H and V_L were previously taken to be the high-and low-frequency band measurements whose ratio is defined to be spectral ratio. Now let V_{H1}, V_{H2} and V_{H3} be the value of the 10-second V_H measured on a beam for the first noise interval, the second noise interval, and the signal interval, respectively. Let V_{L1}, V_{L2} and V_{L3} be similarly defined but in terms of V_L. Thus, for example, V_{H1}/V_{L1} and V_{H2}/V_{L2} would be spectral ratio measurements made on noise only.

We can now define the signal-to-noise factors $\rho_{H1} = V_{H3}/V_{H1}$ and $\rho_{H2} = V_{H3}/V_{H2}$ which are indicative of the extent to which noise might be effecting V_{H3}. The similarly defined quantities ρ_{L1} and ρ_{L2} can be used for the low-frequency band. Figures 16 and 17 show plots of these quantities as a function of LASA magnitude. Each event is represented by a vertical bar with extremes given by (ρ_{H1}, ρ_{H2}) or (ρ_{L1}, ρ_{L2}). The relatively small variations in measured ρ for a given event (typically less than 50%) is accounted for by the stability of the measurements on noise preceding the event. Figure 18 shows histograms for some measurements of V_{H1}/V_{H2} and V_{L1}/V_{L2} which verify this stability.

The signal-to-noise factor is clearly not the same as signal-to-noise ratio. Figure 19 is a plot of 10 log $(\rho^2 - 1)$ vs ρ, which crudely relates the noise factor ρ to the signal-to-noise ratio (SNR). The relationship was obtained by assuming that both the noise and signal spectra are white noise random processes with frequency as the parameter. The figure actually relates the ratio of expected values of the V's to the signal-to-noise ratio. Although the relationship is admittedly crude, it is convenient to be able to relate ρ to a more common parameter such as SNR. For example, $\rho = 3$ is about the same as 9 db SNR and $\rho = 1.4$ is the same as about 0 db SNR.

Since SNR can seriously affect spectral ratio it is necessary to make decisions concerning the validity of spectral ratio measurements. There are four distinct SNR situations. First, if SNR is large in both the high-and low-frequency bands, then the spectral ratio measurement is valid and truly reflects the event characteristics. Second, if the SNR is small in both bands, then the measurement of spectral ratio can lead to incorrect conclusions since the noise properties determine the spectral ratio. Third, if the SNR is poor only in the high-frequency band, then the measured spectral

ratio will be increased from the true value by the noise. Thus if the event appears in the earthquake region with respect to spectral ratio, it would have been in that region even in the absence of noise. However, if the event appears to be in the explosion region, it means no decision should be made. The fourth situation is that in which the SNR is poor only on the low-frequency band. In this case the noise tends to reduce the measured spectral ratio. Events which appear in the explosion region should be accepted since the noise could only depress the spectral ratio. No decision can be made for events which appear to be in the earthquake region.

We have considered SNR large enough if it is greater than 9 db ($\rho \geq 3.0$). Table I summarizes the decision rules which take SNR into consideration if $\rho = 3.0$ is used as a threshold value on the signal-to-noise factor.

Figure 20 shows spectral ratio vs LASA m_b for the events on Fig. 15 which remain after the SNR test is applied. That is, events which appear on Fig. 15 but not on Fig. 20 have SNR values which preclude making a decision based upon spectral ratio. Events on Fig. 20 indicate the true power of spectral ratio as a discriminant since the spectral ratio for those events is only modestly effected by noise. Events indicated by numbers and letters on Fig. 20 are discussed further in Section XII.

Since spectral ratio cannot be applied to all events independent of SNR it is important to know, as a function of m_b, what is the probability that it can be applied. Figure 21 shows this probability under the condition that the event is an earthquake. The data points on the figure are the fractions of events in 0.1 magnitude intervals on Figure 15 which also appear on Fig. 20. The probability can be interpreted as the probability that a good indication of event type will be generated by spectral ratio if noise free spectral ratio is a good discriminant.

TABLE 1

Modified Spectral Ratio Decision Rule

$\rho_H > 3,\ \rho_L > 3$	Accept spectral ratio measurement ρ, and discriminate according to the decision line shown on Fig. 12.
$\rho_H > 3,\ \rho_L < 3$	If ρ indicates explosion, then decide explosion. If ρ indicates earthquake, make no decision.
$\rho_H < 3,\ \rho_L > 3$	If ρ indicates earthquake, then decide earthquake. If ρ indicates explosion, make no decision.
$\rho_H < 3,\ \rho_L < 3$	Make no decision.

It was stated in Section VII that the 10-second spectral ratio was at least as successful as the 20-second spectral ratio as a discriminant. Figure 22 can be compared with Fig. 20 to verify this assertion. The plot of 20-second spectral ratio vs m_b contains all the same points as Fig. 20. The comparison is made on this data set since spurious noise effects have been minimized as much as possible.

IX. LASA PERIOD AS A DISCRIMINANT

It seems that, in the absence of noise, the short-period spectra of events can be used as a discriminant. However, it was demonstrated in the previous section that noise can seriously effect the use of spectral information at small magnitudes. This motivates the consideration of a spectrum related discriminant which might be less effected by noise. Dominant period is a candidate for such a discriminant.

The dominant period of an event is generally defined in terms of the seismogram itself although one normally thinks of it as a spectral property. The relationship between spectrum and dominant period is at best crude and will not be discussed here. We have taken dominant period to be twice the time between the positive and negative parts of the largest peak-to-peak excursions of LASA beams which have been bandpass filtered from 0.6 to 2.0 Hz. SPLP generates the dominant period and is not subject to human subjectivity. Due to the measurement procedure and the LASA sampling rate all dominant periods were reported as multiples of 0.1 seconds.

Figure 23 shows dominant period vs LASA magnitude for all events in our population except those reported at depths greater than 100 km by USCGS. One possible decision line has been drawn which contains all explosions in the lower right section of the plot. This data is similar to that presented previously by Kelly[4] but is more complete and has had some of the human factors removed.

If Fig. 23 is accepted at face value, it suggests that all explosions, even down to below magnitude 4.0, can be correctly indicated but that only 53% of the earthquakes will be correctly identified. However, it also suggests that the quality of a decision based upon period might strongly depend upon magnitude. If attention is directed to the important range below magnitude 4.5, we observe that all explosions are correctly

identified and 72% of the earthquakes are correctly identified. If such performance is actually possible, then dominant period can be a valuable discriminant in the low magnitude range.

Before terminating this section, it is important to note that dominant period as well as spectral ratio may be highly dependent upon the receiver location as well as the source regions. The properties of spectra in the low-and high-frequency bands as well as dominant period may be very different for another receiver even for the same source regions.

X. LASA COMPLEXITY AS A DISCRIMINANT

The value of complexity as a discriminant has been quite extensively discussed by Kelly.[4] He concluded that complexity is of limited usefulness. Our data has substantiated and strengthened that conclusion.

Figure 24 is a plot of complexity vs magnitude for all events except those located at depths greater than 100 km by USCGS. The data contains more large earthquakes and small explosions than have been previously available. It is clear that even for large events (say $m_b > 4.8$), for which there are no noise contamination difficulties, complexity is not a powerful discriminant. A decision line is shown drawn at 3.0 so that all explosions are properly identified. Complexity then correctly identifies only 53% of the large earthquakes and only 47% of all earthquakes. If the decision line is brought down to a complexity of 2.0, the percent of correctly identified earthquakes increases to 73%. However, two explosions are then moved well into the earthquake region. One can probably ignore the small explosion since the background noise is forcing the complexity to be large. The large event cannot be ignored and, as previously pointed out by Kelly, forces retention of the higher decision level which results in poorer performance.

XI. DEPTH PHASES AT LASA

Earthquake depth is an extremely important parameter in any discrimination study. For example, if depth is firmly established to be more than just a few kilometers, an event can obviously be identified as an earthquake. In addition, certain other discriminants, such as complexity, dominant period, spectral ratio or the $M_s - m_b$ relationship, are generally believed to be a function of depth. Indeed, deep events (> 100 km) often generate very small surface waves and often have teleseismic P waves very much like those of underground explosions.

All events in our population have been examined by an analyst for possible depth phases (sP or pP). The analyst operated as follows. First the SPLP beam waveforms were examined for any possible arrivals after the initial P wave onset. Picks corresponding to PcP times were discarded. The time corresponding to the largest amplitude of any remaining picks was then accepted as a candidate for sP or pP. The analyst accepted picks associated with amplitudes less than 25% of the P amplitude only if he felt the arrival very clearly rose above the coda or noise level.

The above procedure was scrupulously executed for presumed explosions as well as for earthquakes. As a result erroneous depth phases were attributed to three explosions in the population. Two of these were complex Novaya Zemlya events with many apparent secondary arrivals, some as large as 0.8 of the initial P amplitude. The third event was quite simple and is shown as event 2 in Fig. 26.

The danger of accepting apparent depth phases at LASA as unequivocal evidence of depth for discrimination is obvious. Corroborating evidence from other sources should be required in order to avoid the incorrect classification of an explosion as an earthquake.

The analyst accepted depth phases for 58% of all the earthquakes in our data base. This is just slightly less than the acceptance rate for the 55% of all earthquakes in the data base which were also reported by USCGS. For that subset of earthquakes depth phases were attributed to 63% of the events by the analyst.

If events restrained to 33 km by USCGS are excluded from consideration there are 41 earthquakes in our population to which we attributed depth phases and which were reported by USCGS. Figure 25 shows the degree of agreement between USCGS depths and the depths implied by the possible depth phases observed on the SPLP beams. Each event is represented by (1) a vertical line indicating the USCGS confidence interval and (2) a solid dot indicating the SPLP depth which is obtained by assuming the phase is pP. In cases where a depth computed by assuming the phase to be sP gives better agreement with USCGS the sP depth has been indicated by an open dot. In cases where there might be confusion lines connecting dots and vertical lines have been included to indicate that they should be associated with the same event.

Given the available data shown on Fig. 25 it is at least difficult to precisely evaluate the success of the depth determinations made using SPLP. There are only two cases (LASA pP depth = 29 km, USCGS depth = 87 km; LASA pP depth = 80; USCGS depth = 10) in which there is virtually no doubt that the LASA phase was neither pP nor sP. There are about 30 cases in which it is most reasonable to assume that the SPLP phase was either pP or sP. The remaining events are ambiguous at best. Thus, for earthquakes, between 70% and 95% of the possible depth phases picked on SPLP beams corresponded to either sP or pP. This implies that sP or pP was correctly picked for between 42% and 57% of all the earthquakes in our population.

Observe that the decision based upon a possible depth phase is the only one which is in error by incorrectly identifying a presumed explosion as an earthquake. If such an error is very serious, then discrimination based upon depth phases is not acceptable without much more verification than is possible at a single site. However, the fact that all but one of the earthquakes which were problems for spectral ratio appear to have depth phases is suggestive of the worth of depth phases if they can be adequately verified. Because of this problem of the false classification of an explosion we will not consider possible depth phases as a discriminant in the remainder of this section.

It is obvious from Table III that not all discriminants yield the same decision for a given event. Even leaving possible depth phases out of consideration there are clearly disagreements for events C, E, G, I. For example, events C and G are identified as earthquakes by $M_s - m_b$ and as explosions by spectral ratio. Event E is identified clearly as an earthquake by first motion but is clearly indicated to be an explosion by the LASA $M_s - m_b$ criteria. Event I is apparently incorrectly identified by spectral ratio but is correctly identified by complexity. In addition, the first motion may be dilatational although we have not indicated it as such in table III. We hope that these various disagreements adequately demonstrate the multivariat nature of the discrimination problem.

TABLE II

	Symbol of Figs. 20, 22	m_b	M_s*	Complexity	Period	First Motion**	Time to Possible Phase	Spectral Ratio
Earthquakes	A	6.24	4.76	3.1	0.8	–	8	0.39
	B	5.75	4.45	5.0	0.8	+	13	0.45
	C	5.81	4.20	2.6	0.7	+	12	0.79
	D	5.87	5.63	5.7	1.0	+	13	0.39
	E	5.70	3.21	1.6	0.9	–	10	0.40
	F	4.43	<3.53	3.3	0.8	+	11	0.76
	G	4.82	3.09	2.0	0.8	+	5	0.86
	H	5.44	3.64	1.4	0.9	–	–	0.45
	I	4.65	<4.94	3.3	0.8	+	23	1.00
	J	4.91	——	7.1	1.0	+	11	0.63
Presumed Explosions	1	4.69	<2.75	1.59	0.8	+	—	0.77
	2	5.87	3.57	1.38	0.9	+	20	0.42
	3	4.95	<3.30	0.89	0.8	+	—	0.89

* <indicates an upper limit on M_s imposed by noise or an interfering event

** First motion is indicated + if it is + or highly ambiguous.

XII. DETAILED DATA FOR SOME SPECIFIC EVENTS

It is the behavior of individual discriminants which has been considered in the preceding sections. In this section the data from some specific events are used to give some indication that discrimination is not just a one-dimensional problem. The interaction and statistical dependence between various discriminants is of great importance. Although we have not investigated this area in depth it is hoped that our consideration of several discriminants for a few events will serve to indicate how important it is.

Three presumed explosions and 10 earthquakes were singled out on Fig. 20 because they were either incorrectly identified by spectral ratio or were the most marginal events. Figure 26 gives waveform information for those events. The SPLP data is summarized in Table II. Since first motion is obviously important for these events the table includes a column for the polarity of first motion as well as for the discriminants discussed in earlier sections.

Table III shows decisions which might be made using the data in Table II. A decision in favor of the earthquake hypothesis is indicated by "quake." A decision in favor of the explosion hypothesis is indicated by "exp." A blank appears when, in our opinion, the value of the discriminant does not suggest one hypothesis much more strongly than it suggests the other.

The period column of Table III is completely blank. If the period of any of the events had been sufficiently long (see Fig. 23) then an earthquake decision would have been made. However, a short-period, except at magnitudes lower than that of any of the 13 events under consideration, does not significantly reduce the probability that the event is an earthquake. Thus we have decided to indicate no decisions based upon period.

TABLE III

Event Symbol	$M_s - m_b$	Complexity	Period	Spectral Ratio	First Motion	Possible Depth Phase
A	Quake				Quake	Quake
B	Quake	Quake				Quake
C	Quake			Exp		Quake
D	Quake	Quake				Quake
E	Exp				Quake	Quake
F		Quake				Quake
G	Quake			Exp		Quake
H	Quake				Quake	
I		Quake		Exp		Quake
J		Quake				Quake
1						
2	Exp					Quake
3				Exp		

XIII. SUMMARY

The primary LASA digital recordings for nearly 200 events have been analyzed to obtain refined data for a variety of discrimination experiments. Some of the discrimination studies have been completed and are reported in detail in the body of this report. The report has been primarily limited to the evaluation of individual discriminants measured at a single site. In the most general terms our data corroborates the discrimination performance of $M_s - m_b$, spectral ratio, period, and complexity which has been previously reported by Kelly[4] and Capon, et al.[5]

The ability of LASA to discriminate on the basis of $M_s - m_b$ has been evaluated for those events which did not have other events interfering with the LP data and which were less than about 100 km in depth. One Kuriles earthquake appeared as an explosion unless the USCGS value of m_b was used. Ignoring this one anomalous event LASA discriminated perfectly for events with $m_b \geq 4.8$ in all cases where surface waves were detected. Exclusive of events obscured by other events or for which no usable tape existed, it was possible to observe surface waves for all earthquakes with $m_b \geq 4.8$. All presumed explosions with $m_b \geq 5.1$ could also be identified using their M_s value or the bound imposed by the background noise. Below $m_b \geq 5.1$ no events were unequivocally identified as explosions. However, the probability that an earthquake could be identified as such decreased to zero only gradually as m_b was reduced from 4.8 to about 4.0.

The spectral ratio criteria has been modified to utilize estimates of the signal-to-noise ratio in the bands used to construct the spectral ratio. The modification introduces the option to make no decision. The probability that no decision is made is zero for magnitudes above about 4.8 and unity below about 4.0. Once a decision is made,

the probability that it is correct, given that events deeper than 100 km are excluded, is very high.

Period, plotted against m_b, may be a discriminant which will be valuable at low magnitudes (say below 4.5). It has not been possible to unequivocally identify events as explosions using period. However, many earthquakes with magnitudes below 4.5 can be identified correctly using the period data.

Event complexity measured at LASA appears to be a relatively weak discriminant. Noise effects negate its value for small events. Large events tend to be identified by $M_s - m_b$, spectral ratio, and depth phases. Of course all non-trivial discriminants should play a role in multi-variate or multi-station discrimination. Complexity may occasionally be of more value in that context.

Possible depth phase picks have been made for about 60% of the earthquakes in our population. A comparison with USCGS depths has indicated that between 70% and 95% of the picks are valid depth phases. Unfortunately, depth phases were also picked for three presumed explosions.

All of our data is from a single array station monitoring a limited part of the world. The evaluation of discriminants is strictly valid only for those conditions. Of course there are general physical explanations why the various discriminants should work to some extent. However, the success may vary with site and it may be necessary to significantly modify details to achieve successful operation at different sites. For example, it is anticipated that differences in earthquake and explosion short-period spectra will appear at other sites such as NORSAR, but that spectral ratio as presently defined may not make the most effective use of those differences.

ACKNOWLEDGEMENT

The author wishes to acknowledge the value to him of many interesting discussions with Dr. E. J. Kelly and the very constructive criticisms of this report by Mr. H. W. Briscoe and Dr. P. E. Green. Mr. L. Lande has contributed as an analyst and was directly responsible for many of the computer runs which have been required. In general, the author has benefited considerably from all of the members and facilities of the Seismic Discrimination Group during the preparation of this report.

APPENDIX A

FREQUENCY DOMAIN FILTERING OPERATIONS

All bandpass and chirp filtering operations mentioned in this report were accomplished using Discrete Fourier Transforms (DFT). In this Section we briefly describe the DFT and the filtering procedure which has been used. Extensive expositions of the DFT and its properties are readily available in the literature.

Let $s(n)$, $n = 0, 1, \ldots, N-1$ be samples of a seismogram which we wish to filter. The DFT of this sequence is defined as

$$S(k) = \sum_{n=0}^{N-1} s(n)\ e^{-i2\pi(nk/N)} \quad .$$

It is assumed that k takes on integer values only. The function $S(k)$ is periodic with period N. That is,

$$S(-k) = S(N-k) \quad .$$

If the sequence $s(n)$ is periodically extended outside the interval $[0, N-1]$ by the relation

$$s(-n) = s(N-n)$$

then $s(n)$ is obtained from $S(k)$ by inverse transformation according to

$$s(n) = \frac{1}{N} \sum_{k=0}^{N-1} S(k)\ e^{i2\pi(nk/N)} \quad .$$

Suppose that the time between s(n) and s(n + 1) is δ seconds. That is, s(n), $n = 0,\ldots,N-1$ can be considered as a sequence of samples taken every δ seconds from a seismogram. The Nyquist frequency for this case is $1/2\delta$ cycles per second. Using this, one can associate the integer argument of a DFT on the interval $[0, N-1]$ with real time positive and negative frequencies. Specifically

$$f_k = \frac{k}{N\delta}$$

for $k = 0, 1,\ldots,N/2-1$ and

$$-f_k = \frac{N-k}{N\delta}$$

for $k = N/2+1,\ldots,N-1$.

A simple but effective bandpass filter can be applied to s(n) by setting all S(k) to zero for k which correspond to frequencies outside of the band. For example, let f_H and f_L be the high and low edge of the band. Define $k_H = N\delta f_H$ and $k_L = N\delta f_L$. We assume that k_H and k_L are positive, are founded to the nearest integers, and that $k_H \ll N/2$. The bandpassed signal is now obtained as

$$b(n) = \frac{1}{N} \sum_{R=k_L}^{k_H} S(k)\, e^{i2\pi(nk/N)} + S(N-k)\, e^{i2\pi[n(N-k)/N]} .$$

Because s(n) is real it follows that b(n) is real also.

Except for modifications due to the periodicity of S and periodic extension of s the DFT behaves in many ways like the ordinary Fourier transform. In particular, multiplication of functions in the frequency domain corresponds to convolution in the

time domain. We shall refer to the inverse transform of the frequency characteristic of any filter as the impulse response. We have only considered filters with frequency functions H(k) which satisfy H(k) = H(N-k) so their impulse responses are real. Thus b(n) above can be obtained by convolving the periodically extended s(n) with the impulse response

$$h(n) = \frac{1}{N} \sum_{k=K_L}^{k_H} e^{i2\pi(nk/N)} + e^{i2\pi[n(N-k)/N]}$$

The function h(n) is shown in Fig. 27 for N - 2048, $\delta = 1.0$, $f_H = 0.055$ and $f_L = 0.025$. These parameters were used when filtering long-period data. Because h(n) introduces no phase distortion, it is symmetrical about n = 0 as well as periodic with period N. The impulse response is essentially zero outside of the time interval shown.

Chirp filters[13] are most often considered in the time domain in terms of their impulse response. However, the fast algorithms for DFT make it desirable to perform chirp filtering operations in the frequency domain. We have done chirp filtering using frequency response functions

$$G(k) = \begin{cases} e^{i2\pi(C/N)\,(k-k_o)^2}, & \text{if } k_L \leqq k \leqq k_H \\ e^{-i2\pi(C/N)\,(N-k-k_o)^2}, & \text{if } N-k_H \leqq k \leqq N-k_L \\ 0, & \text{otherwise} \end{cases}$$

Such a frequency function will pass energy in the band implied by k_L and k_H while rejecting energy outside the band. The phase shift through the band is quadratic with

frequency. There will be zero phase shift, resulting in zero delay, of the frequency component $f_o = N\delta k_o$. Such a frequency function does not exactly correspond to the usual chirp filter impulse response, which is a burst of sine wave with linearly changing frequency. This is not of any real importance as long as C can be adjusted to achieve from G a filter reasonably matched to the waveforms of interest (Dispersed Rayleigh wave trains).

Figure 28 shows impulse responses corresponding to two typical values of C which have been used. The zero delay frequency used is 0.05 Hz and N = 2048 with δ = 1.0 second. The upper and lower bandpass frequencies are 0.055 Hz and 0.025 Hz respectively. Outside the time interval shown the waveforms have even smaller amplitudes than at the edges. The amplitude outside the interval shown can be considered to be zero.

APPENDIX B

Each record of the composite event tape contains exactly 4131 four-byte words. The records can be directly read by a binary read in a Fortran IV program operating in an IBM 360 system. Each word of the record is properly interpreted in the program as either an integer or a floating point number as indicated in the following tabular description of the records on the tape. All data is as determined by LASA and SPLP.

WORD	TYPE (INTEGER OR FLOATING POINT)	DESCRIPTION
1	I	Arbitrarily assigned event number. Numbers in the 1500 to 1999 range are possible explosions
2-7	I	Hour, minute, second, tenths of seconds, day number, and year for event arrival at the center of LASA. For impulsive events this is the time of peak excursion. For others, it is an approximate onset time.
8	F	Zero-to-peak amplitude of P wave (mμ)
9	F	Period of P wave (seconds)
10	F	Magnitude
11	F	P-wave azimuth
12	F	P-wave horizontal phase velocity

WORD	TYPE (INTEGER OR FLOATING POINT)	DESCRIPTION
13	F	Latitude (degrees N)
14	F	Longitude (degrees E)
15	F	Distance (degrees)
16	I	This word is set to unity if the peak excursion of the SP P-wave is more than 2.5 seconds after onset; otherwise this word is zero.
17	F	This is the surface factor
18	I	This word is zero if a good surface wave wave detection was achieved. It is unity if normal LP background noise obscured the event. It is two if surface waves from another event obscured the event of interest. Any other value implies that either no LP data was available or equipment errors made it unusable.
19	F	This word is zero unless a possible depth phase was picked. In that case it equals the moveout to the possible phase (seconds).
20	I	Number of 0.05 second digital samples before the time given in words 2 – 7 to the start of the complexity measurement interval.
21	F	Complexity
22	I	Number of samples before the time given in words 2 – 7 to the beginning of the interval used for the measurement of spectra and spectral ratio.
23	F	Spectral ratio measured using a 10-second interval of data.

WORD	TYPE (INTEGER OR FLOATING POINT)	DESCRIPTION
24	F	Spectral ratio measured using a 20-second interval of data.
25-30	I	Hour, minute, second, tenth of seconds, day number, and year for the first sample of the short-period beam.
31	I	Number of 0.05 second samples in the beam (NBM)
32-2079	F	The best unfiltered short-period beam. Data after the first NBM samples are set to zero.
2080	I	One less than the number of 0.05 second samples in the interval transformed to obtain a spectrum for 10 seconds of data (NSPR10).
2081-3105	F	Voltage spectrum using 10-second window on the data. Data after the first NSPR10 is set to zero. Frequencies range from 0.0 to 10.0 Hz in increments of 10.0/NSPR10.
3106	I	Same as 2080-3105 but for a 20-second interval of data.
3107-4131	F	

REFERENCES

1. Seismic Discrimination, Semiannual Technical Summary Report, Lincoln Laboratory, M. I. T., 31 December 1966, p. 7.

2. E. W. Carpenter, "Teleseismic Methods for the Detection, Identification and Location of Underground Explosions," VESIAC Report 4410-67-X, University of Michigan, April 1964.

3. Seismic Discrimination, Semiannual Technical Summary Report, Lincoln Laboratory, M. I. T., 30 June 1967, p. 5.

4. E. J. Kelly, "A Study of Two Short-Period Discriminants," M. I. T., Lincoln Laboratory Technical Note 1968-8, 12 February 1968.

5. J. Capon, R. J. Greenfield and R. T. Lacoss, "Long-Period Signal Processing Results for Large Aperture Seismic Array," M. I. T., Lincoln Laboratory Technical Note 1967-50, 15 November 1967.

6. Seismic Discrimination, Semiannual Technical Summary Report, Lincoln Laboratory, M. I. T., 31 December 1967, p. 3.

7. R. C. Liebermann, et al, "Excitation of Surface Waves by the Underground Nuclear Explosion Longshot," J. Geophys. Res., 71, September 1966.

8. R. C. Liebermann and P. W. Pomeroy, "Excitation of Surface Waves by Events in Southern Algeria," Science, 156, 26 May 1967.

9. J. N. Brune, A. Espinosa and J. Oliver, "Relative Excitation of Surface Waves of Earthquakes and Underground Explosions in the California-Nevada Region," J. Geophys. Res., 68, June 1963.

10. B. Gutenberg and C. F. Richter, "Magnitude and Energy of Earthquakes," Ann. Geophys., 9, 1956.

11. S. S. Alexander and D. B. Rabenstine, "Detection of Surface Waves from Small Events at Teleseismic Distances," Seismic Data Laboratory Report No. 175, 1 March 1967.

12. B. Gutenberg, "Amplitude of Surface Waves and Magnitudes of Shallow Earthquakes," Bull. Seism. Soc. Am., 35, 1945.

13. J. R. Klauder, et al, "The Theory and Design of Chirp Radars," Bell System Technical Journal, 39, July 1960.

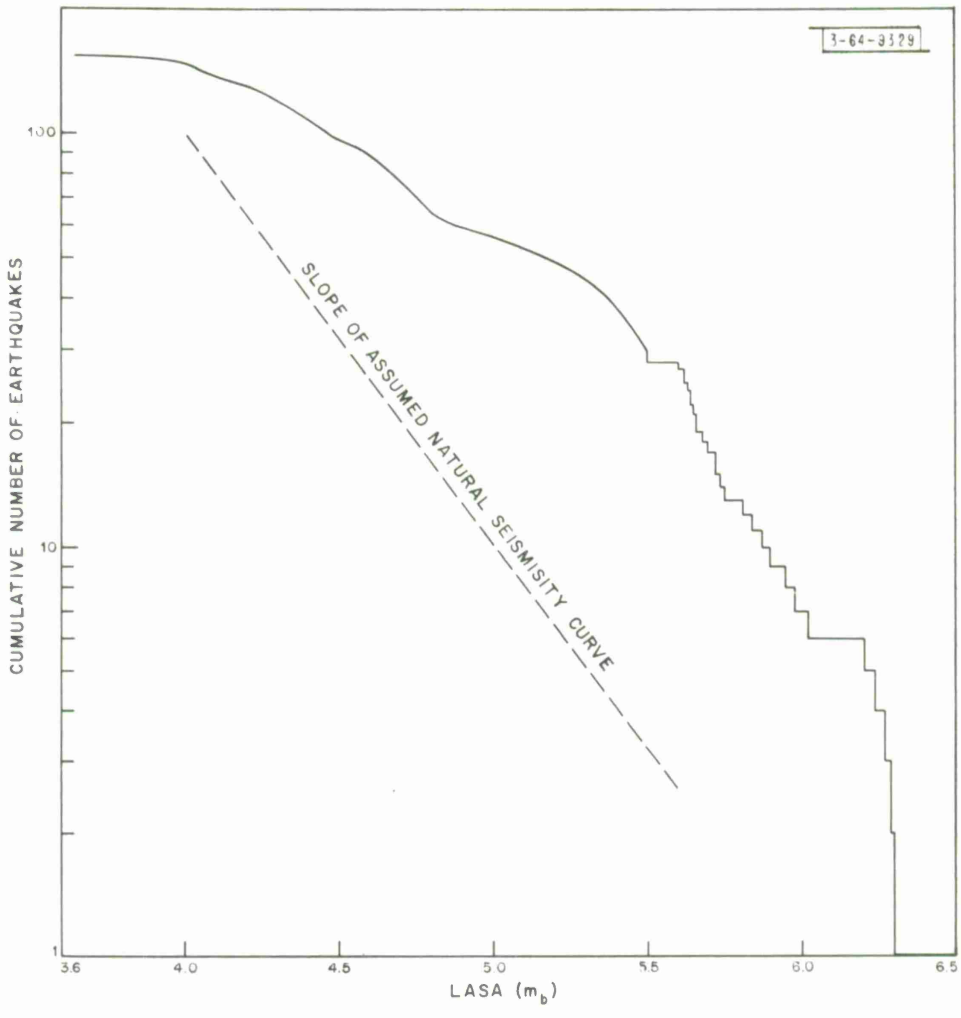

Fig. 1. Body wave magnitude distribution of earthquakes in experiment.

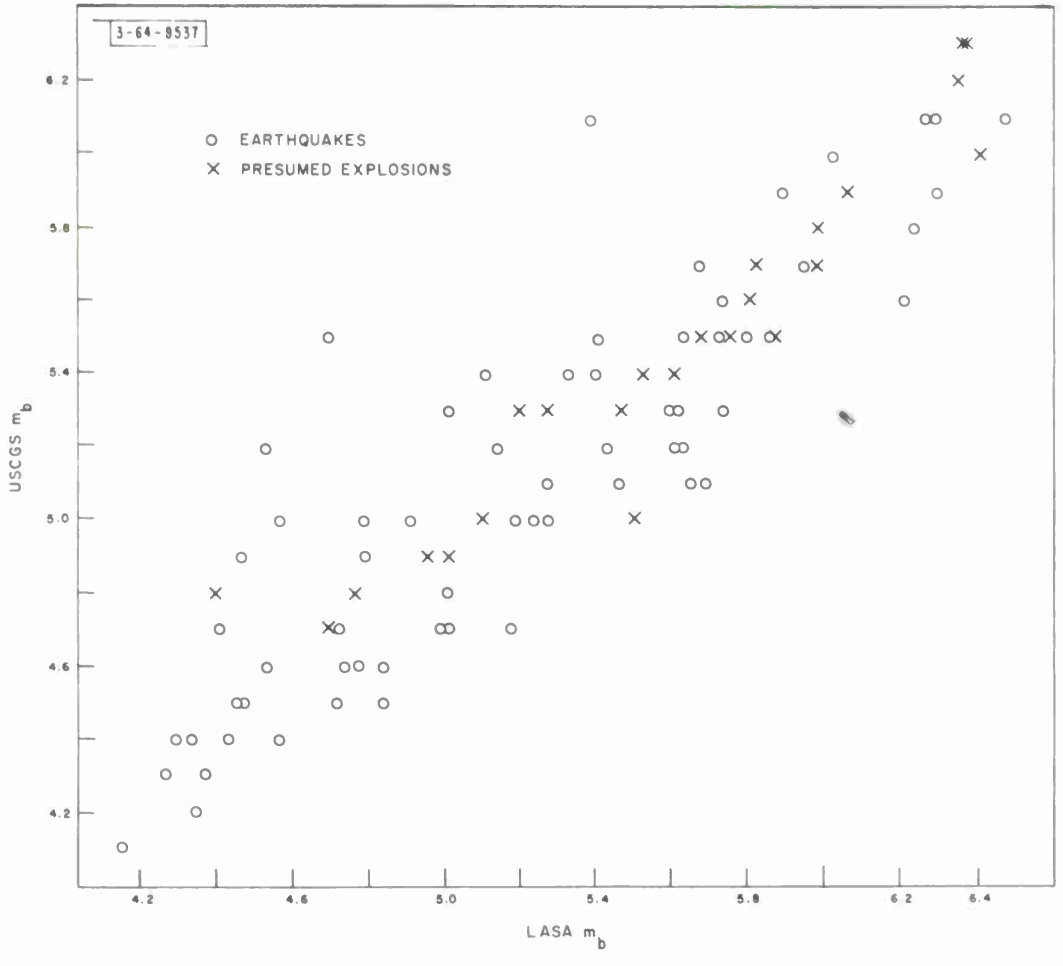

Fig. 2. USCGS m_b vs LASA m_b for events with USCGS depth less than 100 km.

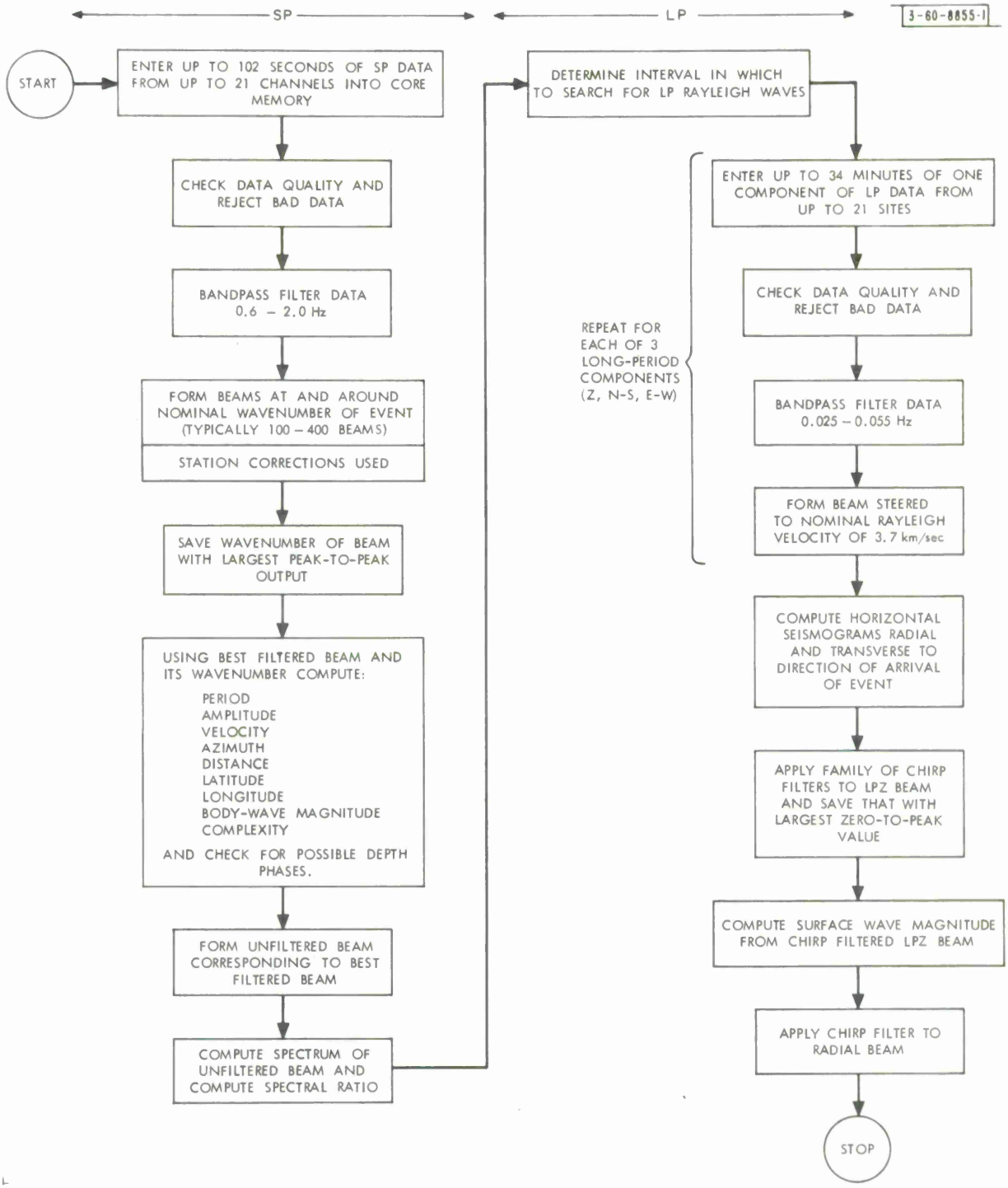

Fig. 3. Sequence of operations in SPLP program.

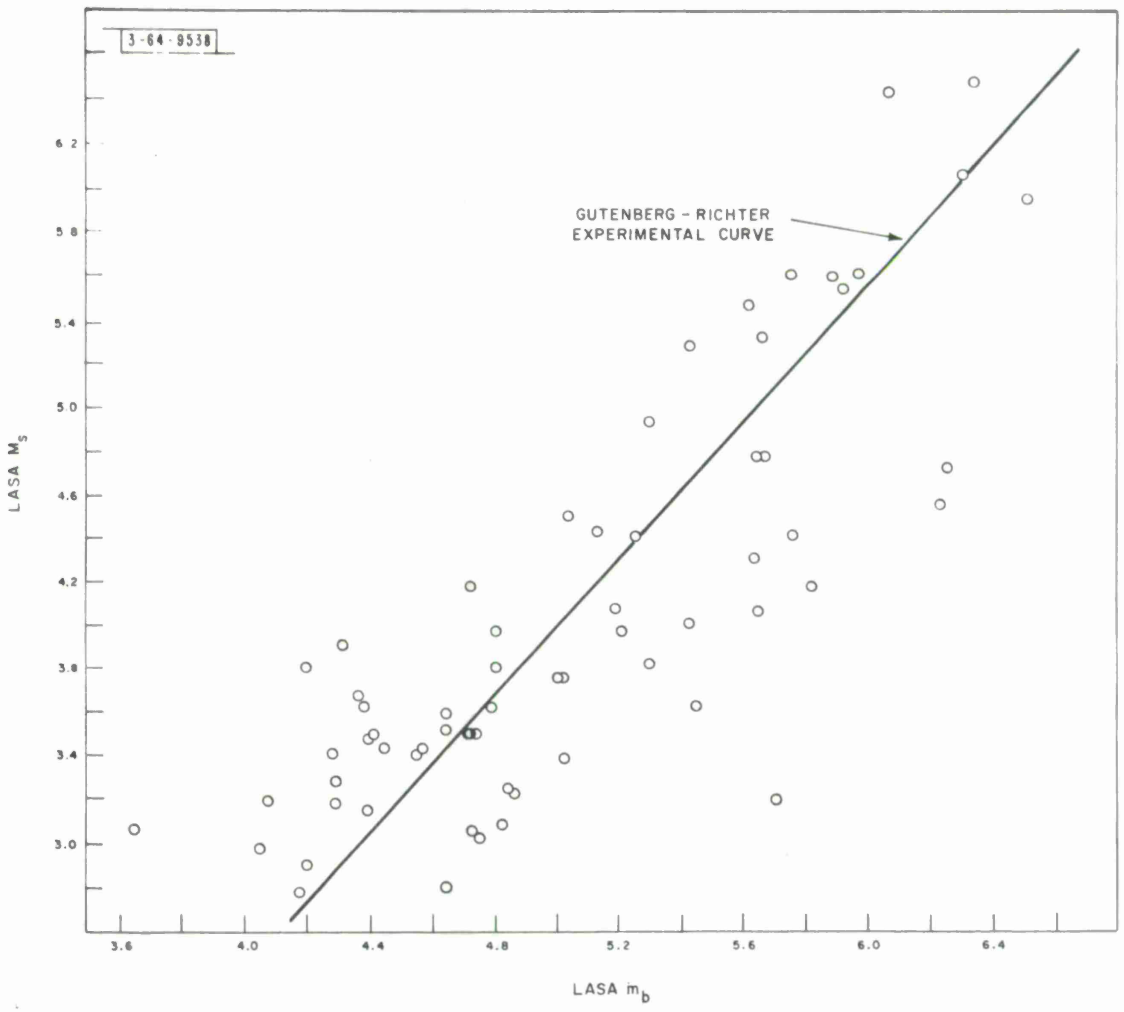

Fig. 4. LASA surface wave magnitude (M_S) vs LASA body wave magnitude (m_b) for earthquakes with detected surface waves (events with USCGS depth $\geq$ 100 km excluded).

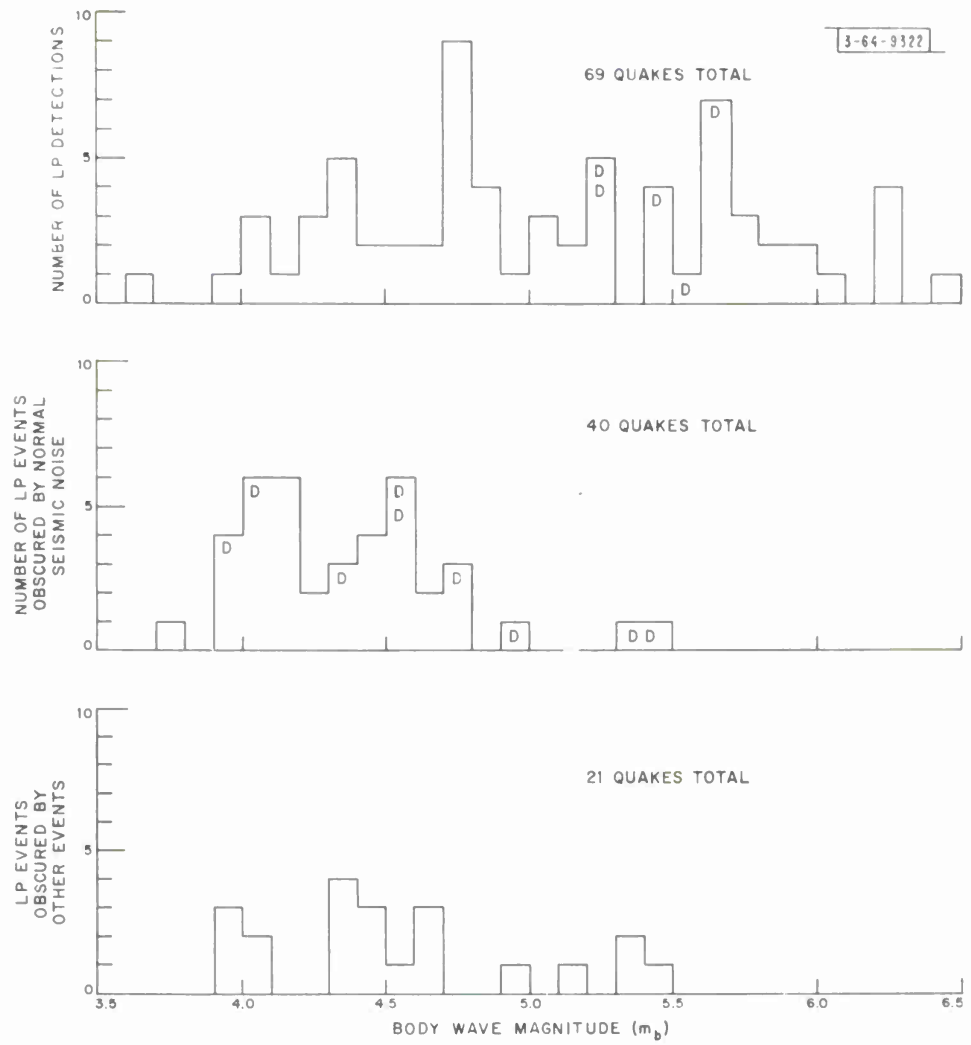

NOTE: D INDICATES DEPTH GREATER THAN 100 KM

Fig. 5. Surface wave detection data for Sino-Soviet earthquakes recorded at LASA.

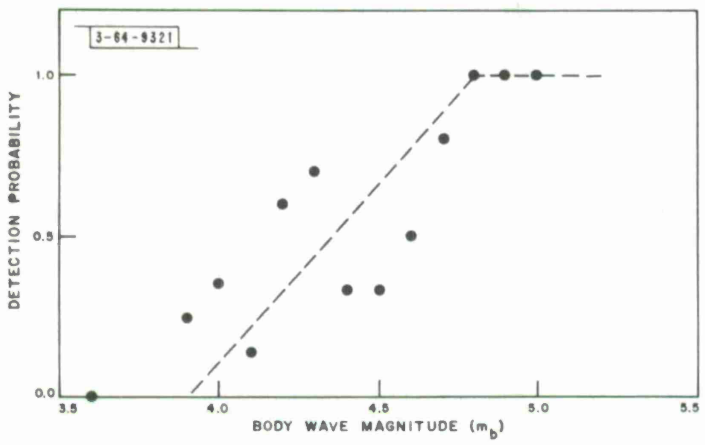

Fig. 6. Surface wave detection probability for Sino-Soviet earthquakes (events with USCGS depth $\geq$ 100 km excluded).

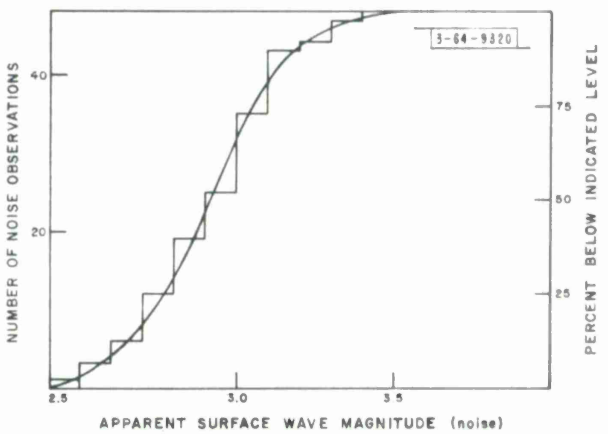

Fig. 7. Apparent surface wave magnitude of long-period noise (Sino-Soviet locations assumed).

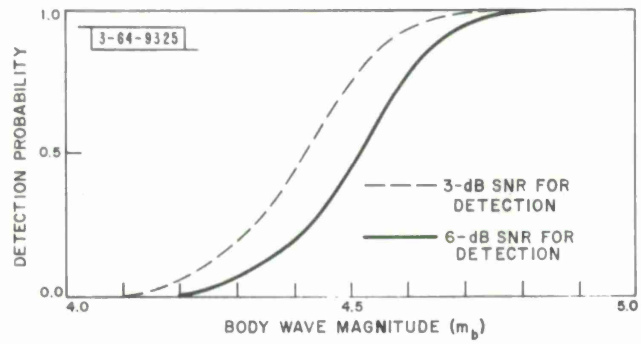

Fig. 8. Surface wave detection probability inferred from noise observations.

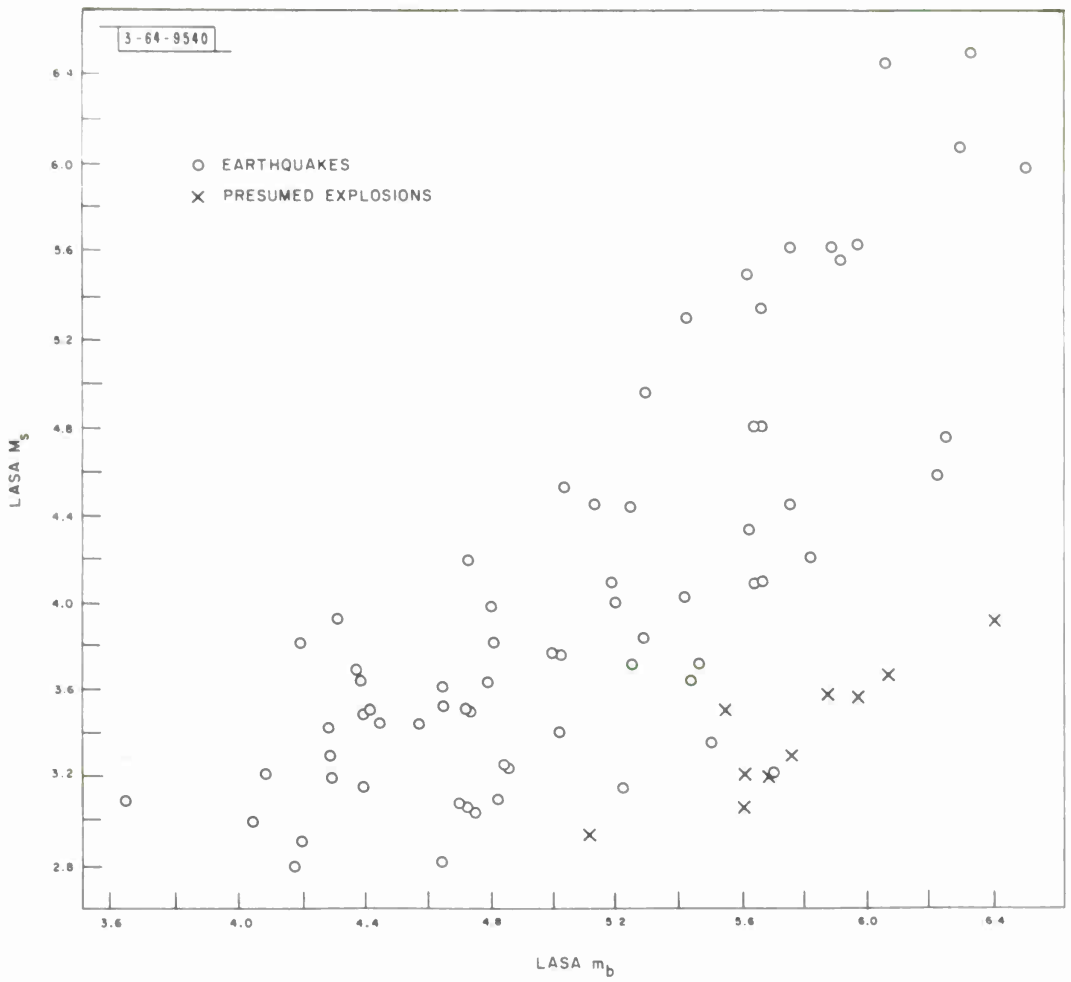

Fig. 9. LASA M_S vs USCGS m_b for all events with detected surface waves.

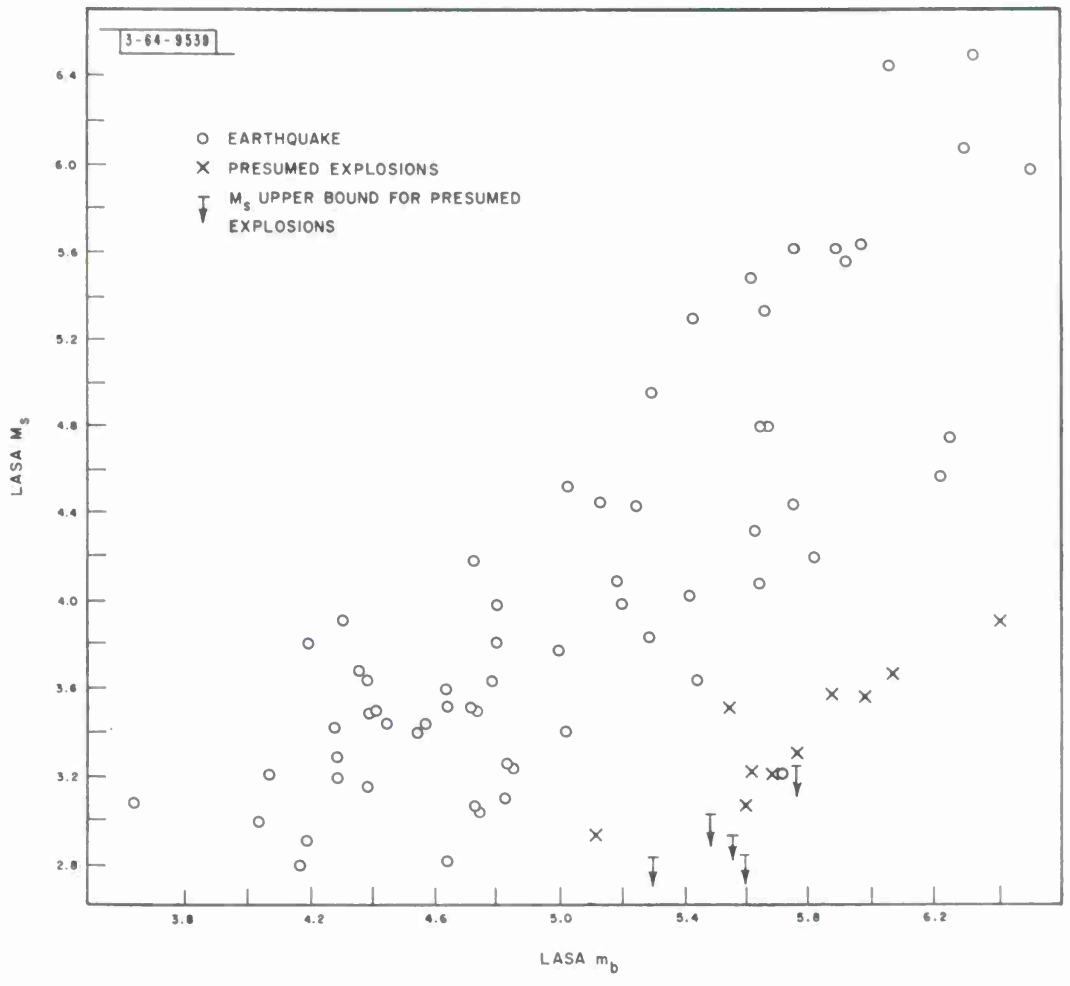

Fig. 10. LASA M_S vs LASA m_b for events with detected surface waves (events with USCGS depth $\geqq$ 100 km excluded).

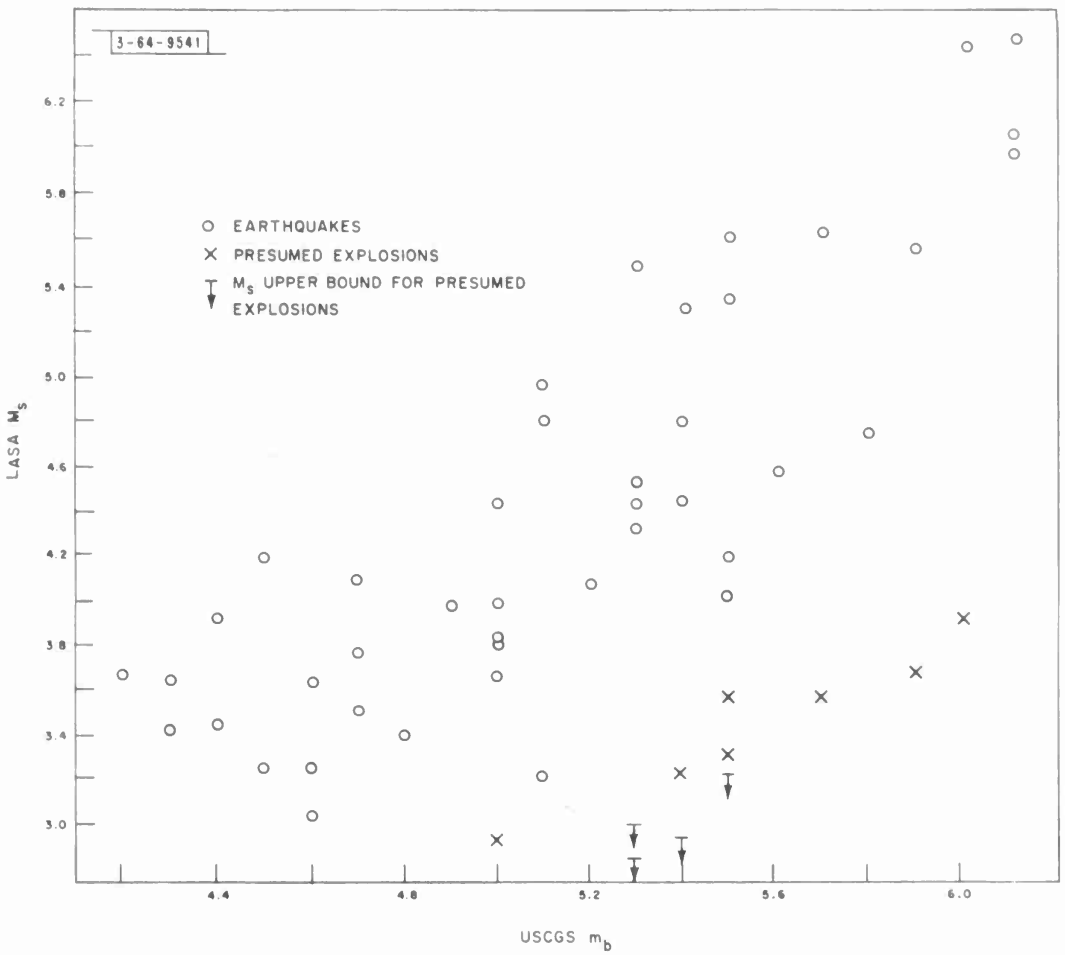

Fig. 11. LASA M_S vs USCGS m_b for detected events with USCGS depth < 100 km.

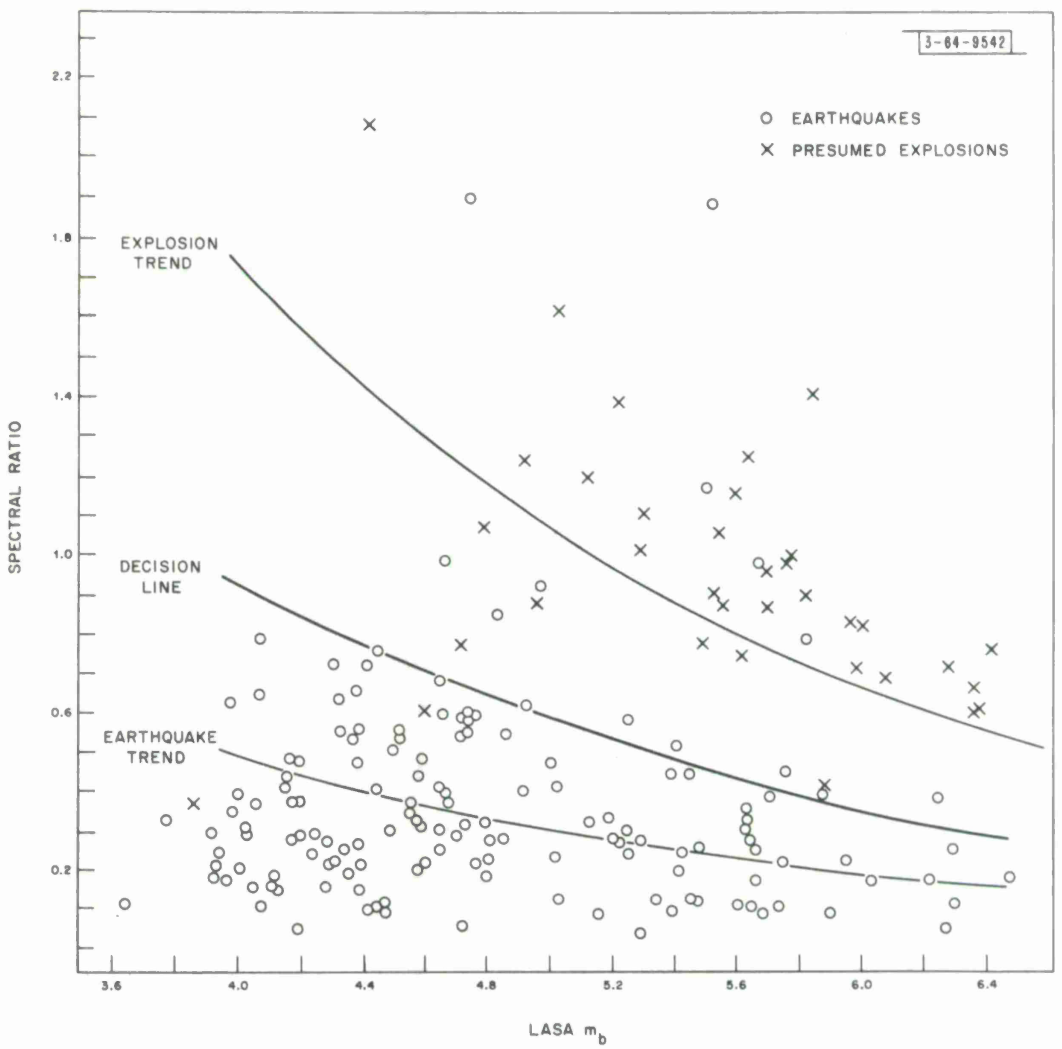

Fig. 12. Spectral ratio vs LASA m_b for all events.

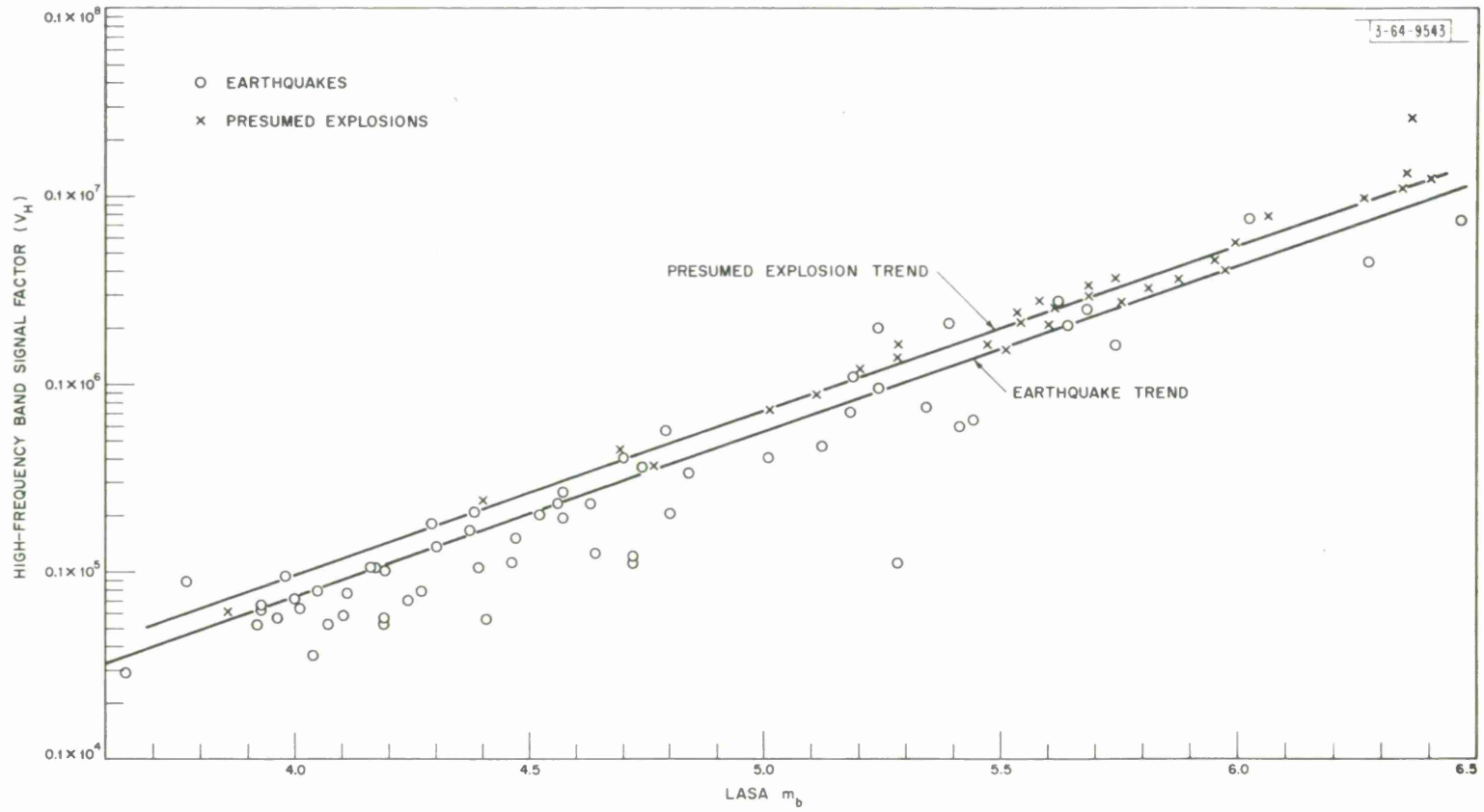

Fig. 13. High-frequency band signal factor vs LASA m_b.

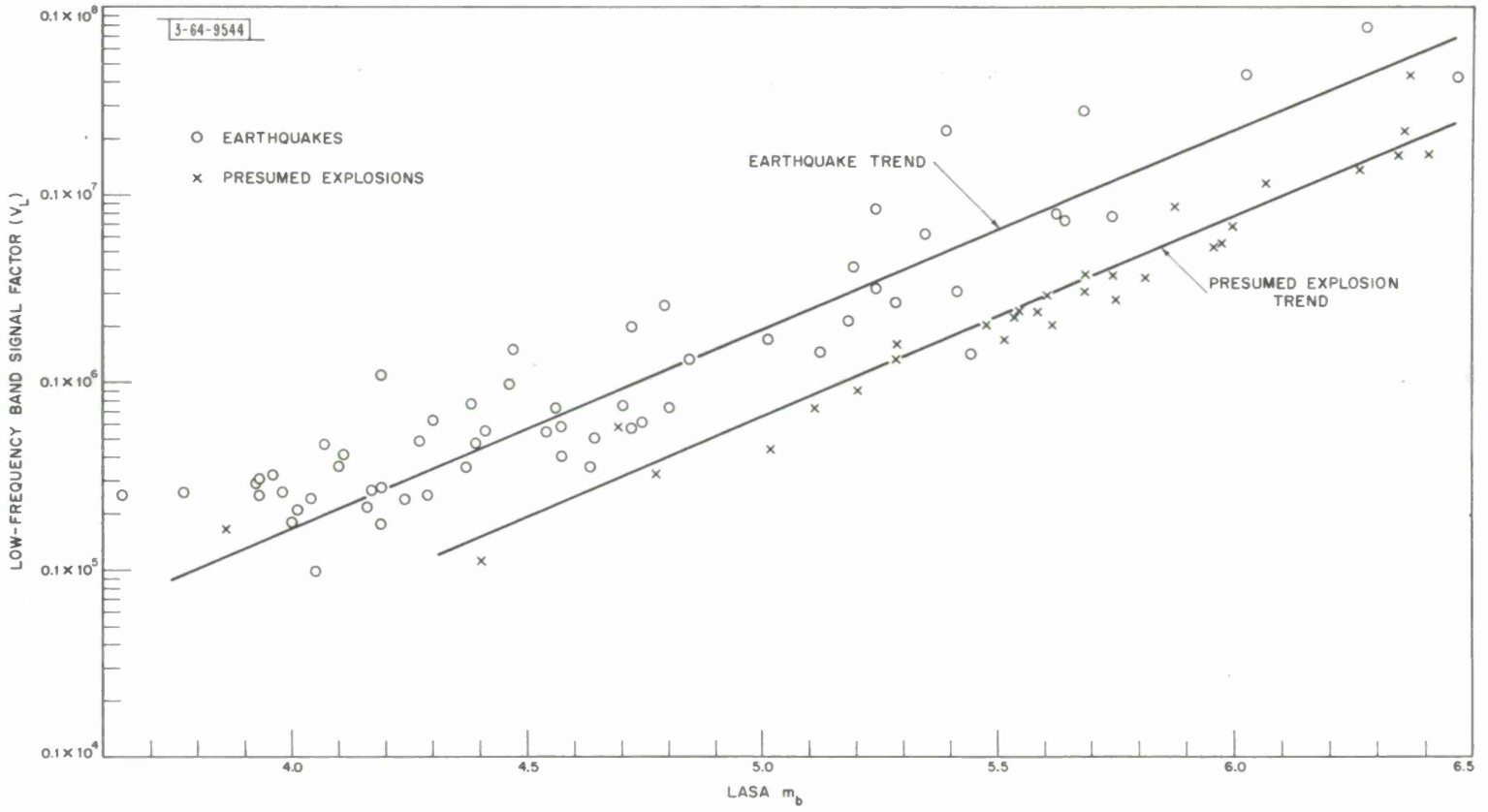

Fig. 14. Low-frequency band signal factor vs LASA m_b.

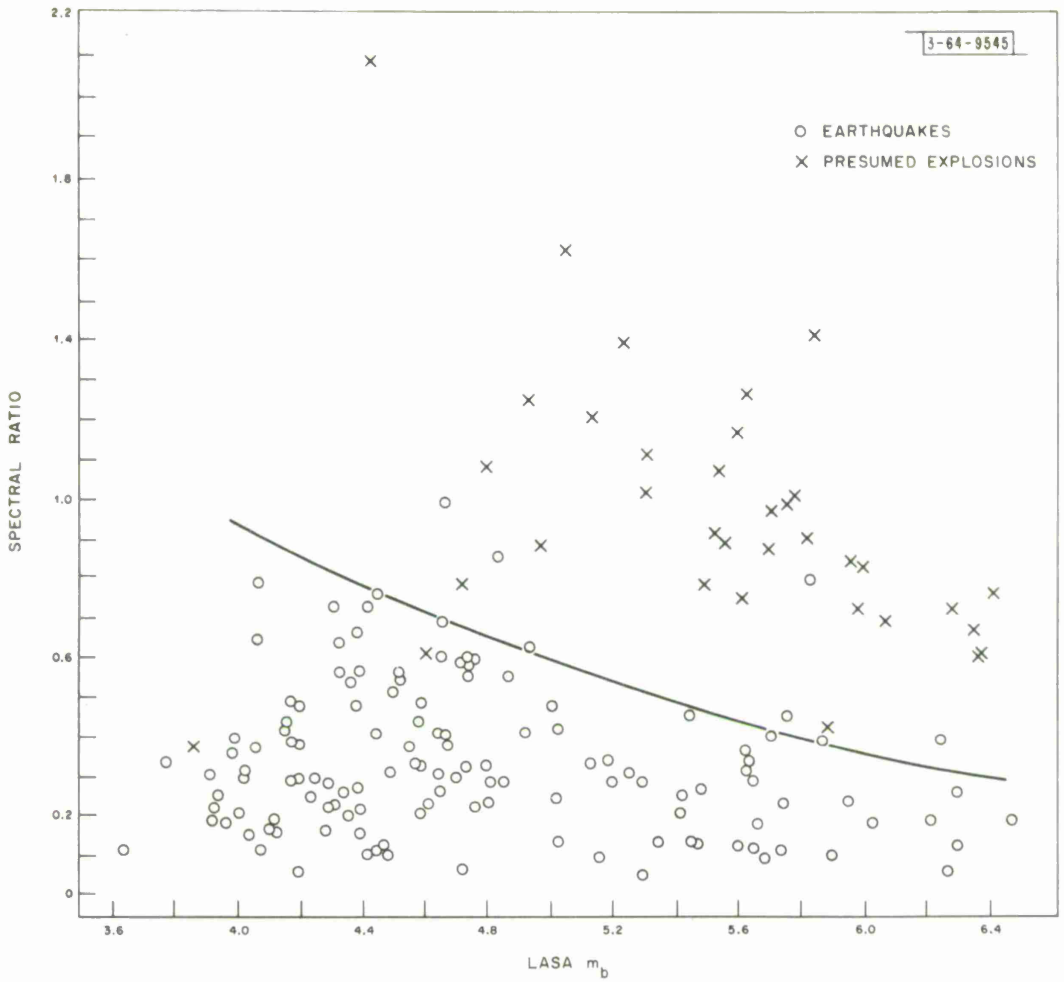

Fig. 15. Spectral ratio vs LASA m_b (events with USCGS depth $\geqq$ 100 km excluded).

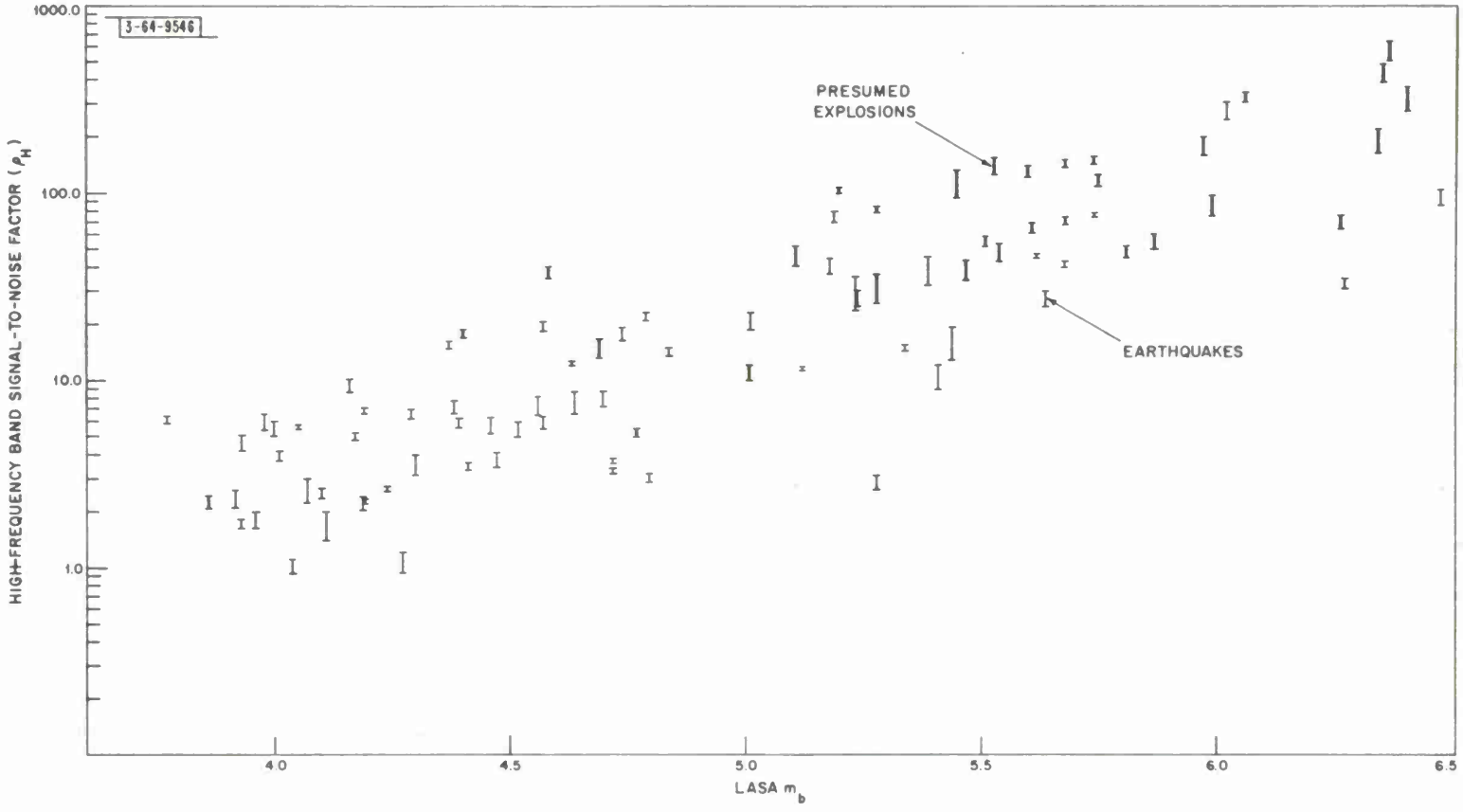

Fig. 16. High-frequency band signal-to-noise factor vs LASA m_b.

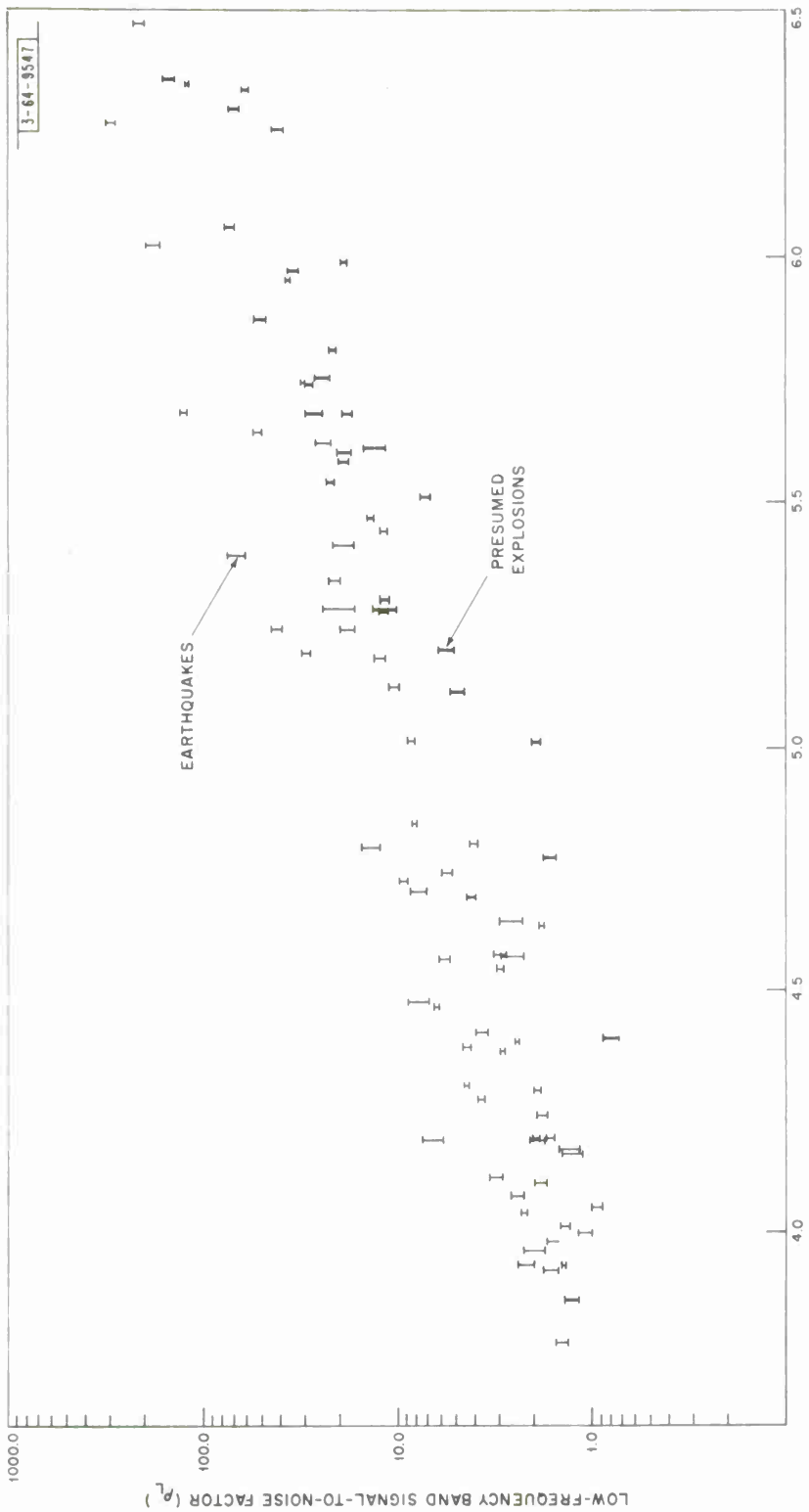

Fig. 17. Low-frequency band signal-to-noise factor vs LASA m_b.

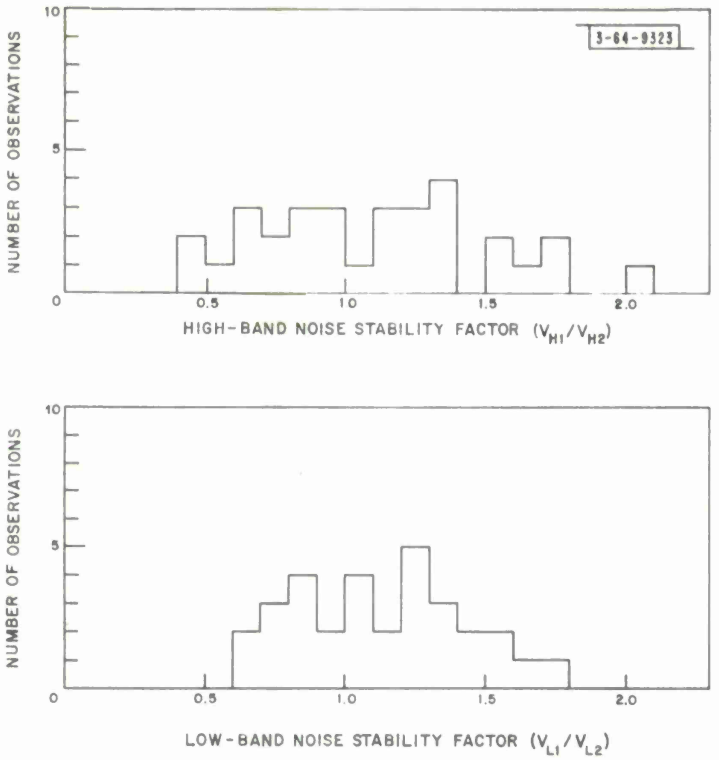

Fig. 18. Stability study for signal-to-noise factor test.

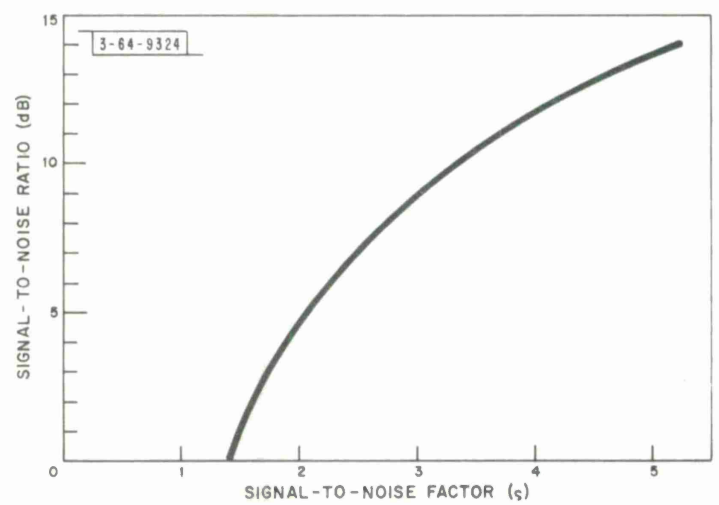

Fig. 19. Signal-to-noise ratio as a function of signal-to-noise factor.

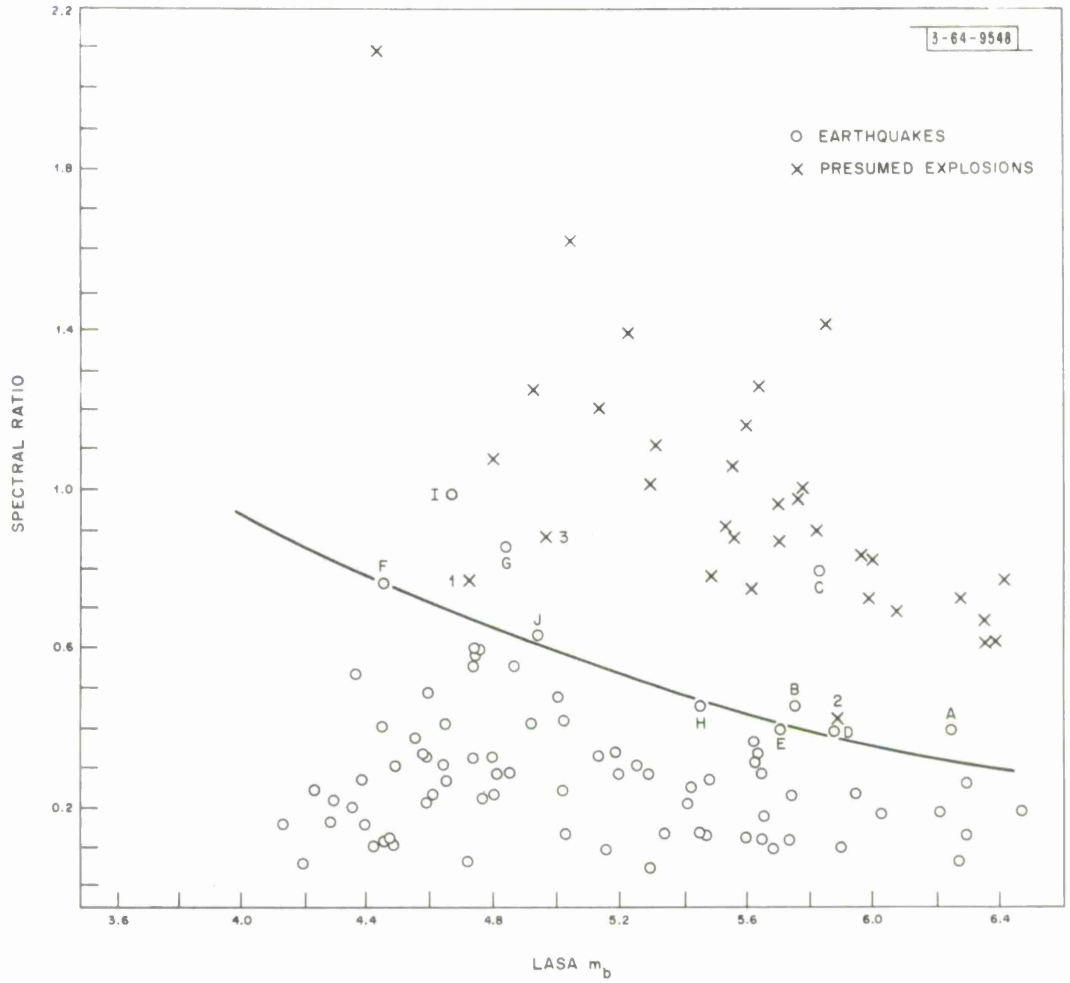

Fig. 20. Spectral ratio vs LASA m_b for events admitted by signal-to-noise ratio test (events with USCGS depth $\geqq$ 100 km excluded).

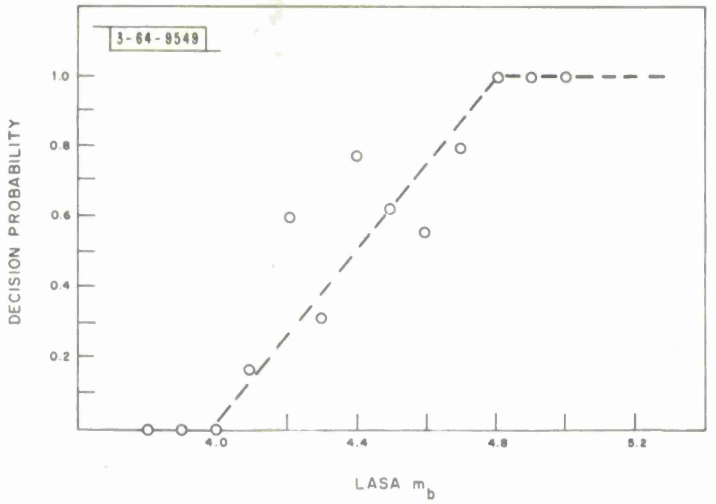

Fig. 21. Decision probability for modified spectral ratio test.

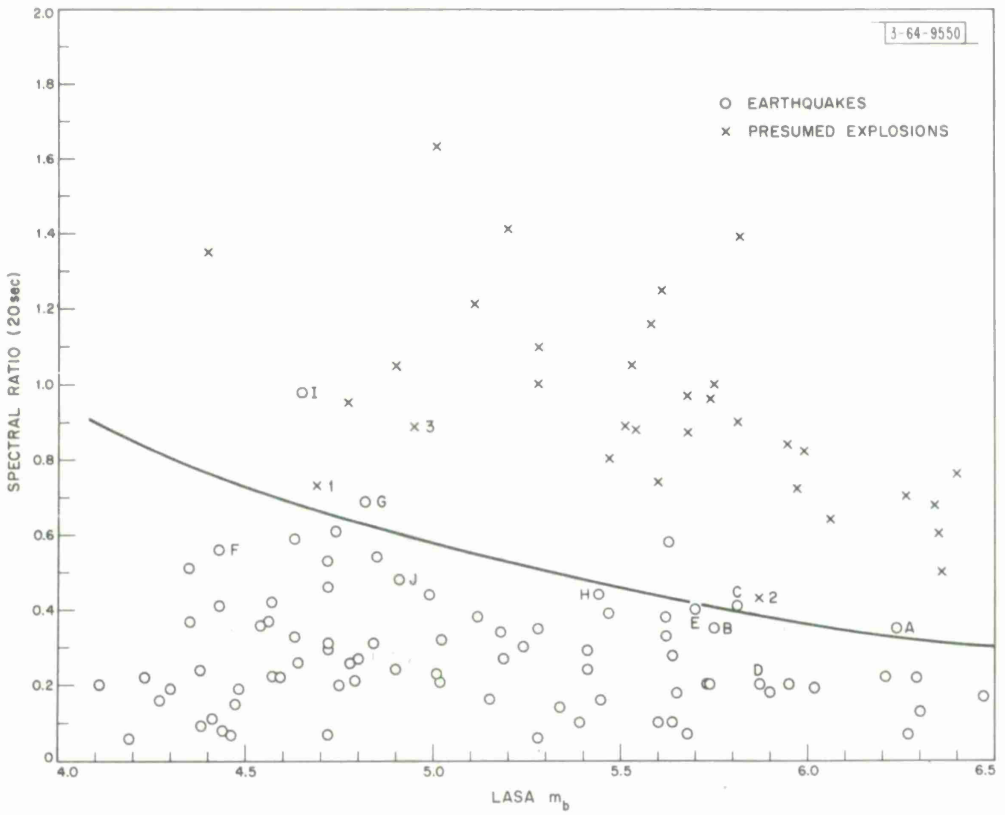

Fig. 22. Spectral ratio from 20 seconds of data vs LASA m_b. (Same events as Fig. 21.)

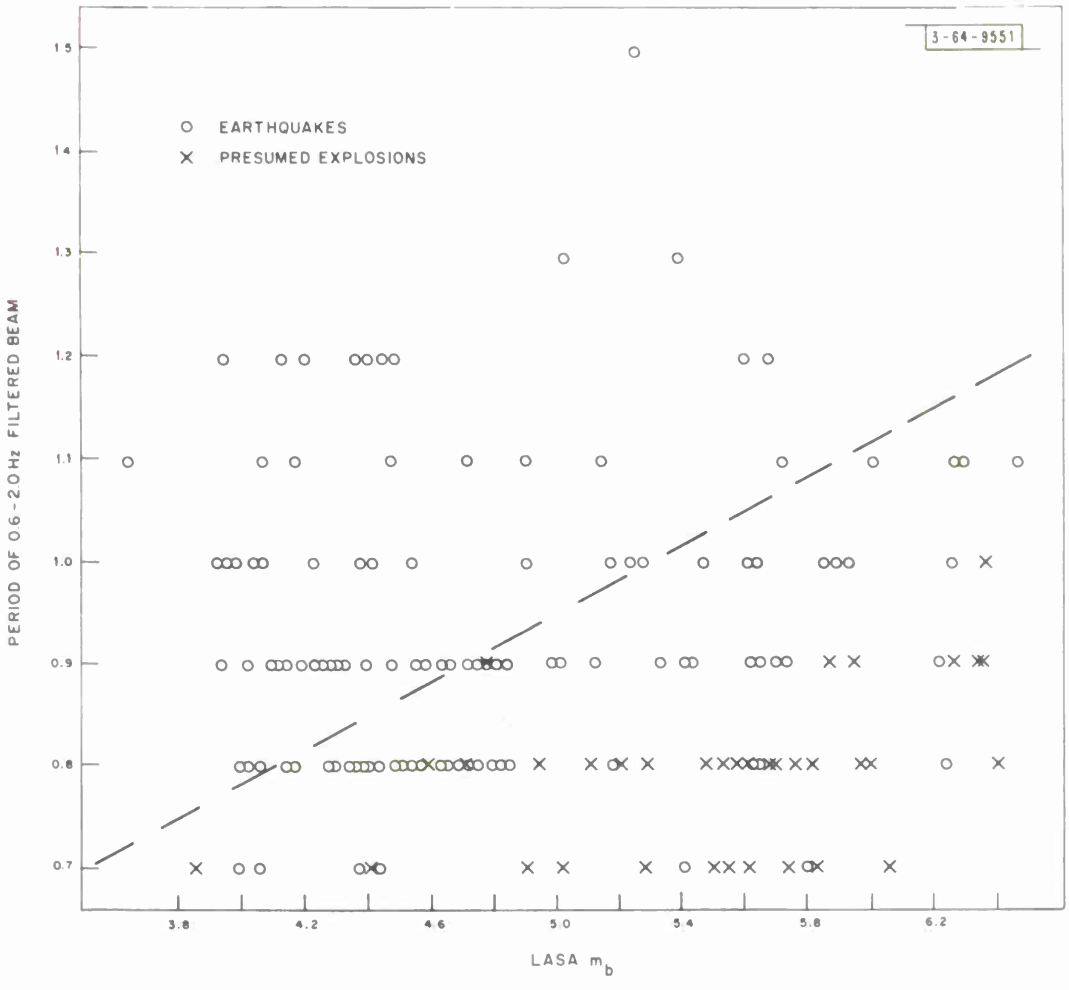

Fig. 23. Period of 0.6 - 2.0 Hz filtered beam vs LASA m_b (events with USCGS depth $\geq$ 100 km excluded).

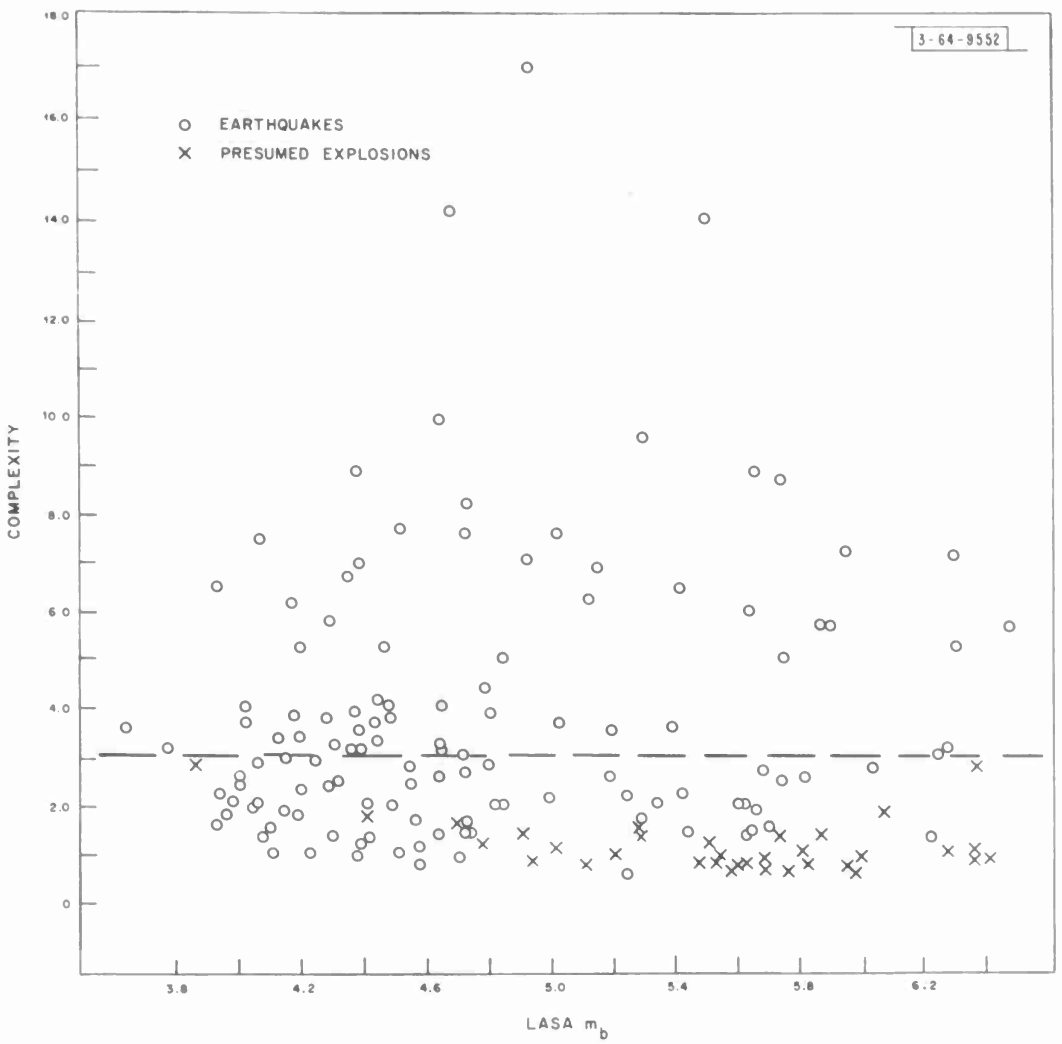

Fig. 24. Complexity measured on 0.6 - 2.0 Hz filtered beam vs LASA m_b (events with USCGS depth $\geqq$ 100 km excluded).

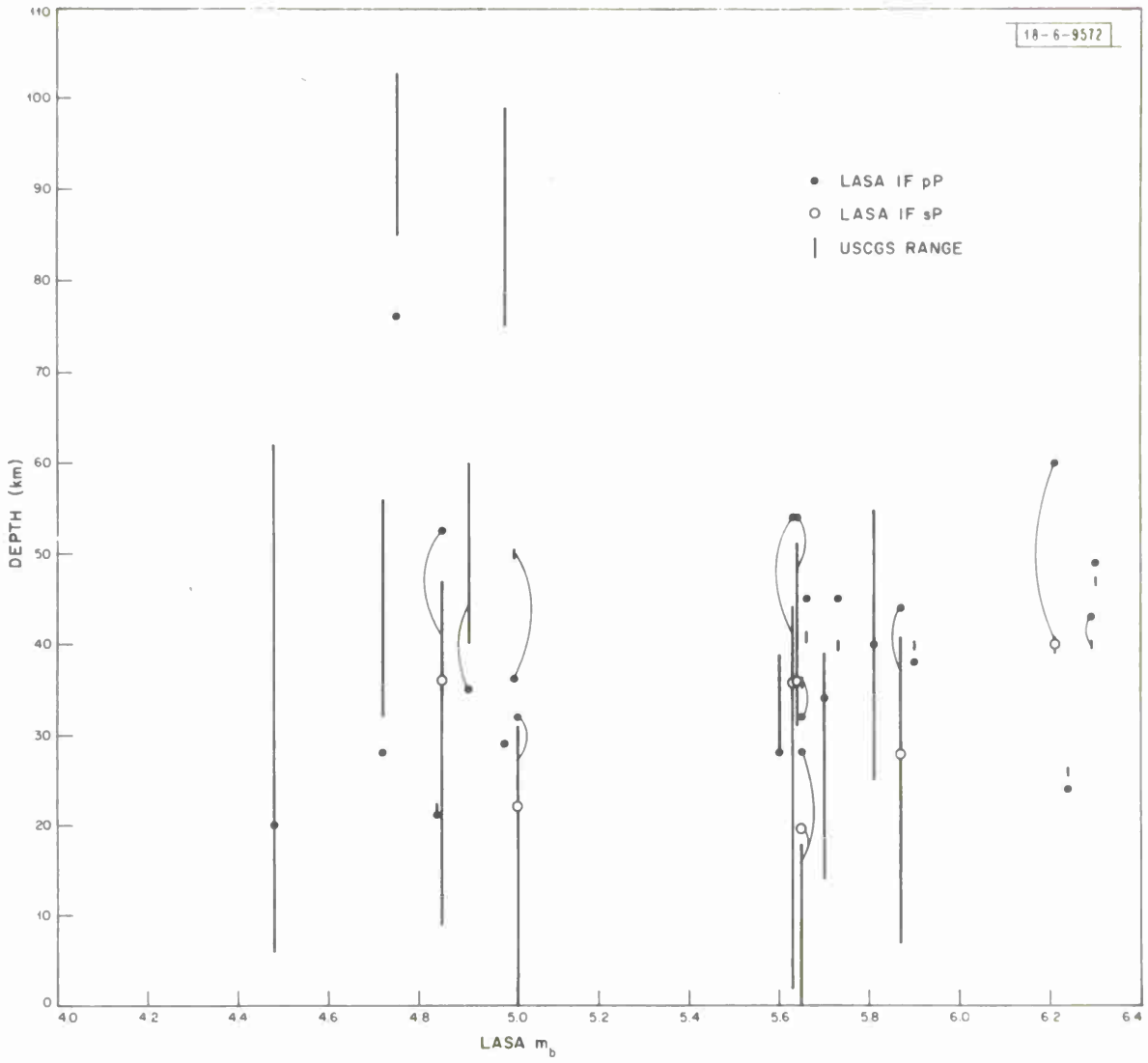

(a) Shallow events.

Fig. 25. USCGS depth vs LASA depth for earthquakes with possible depth phases at LASA.

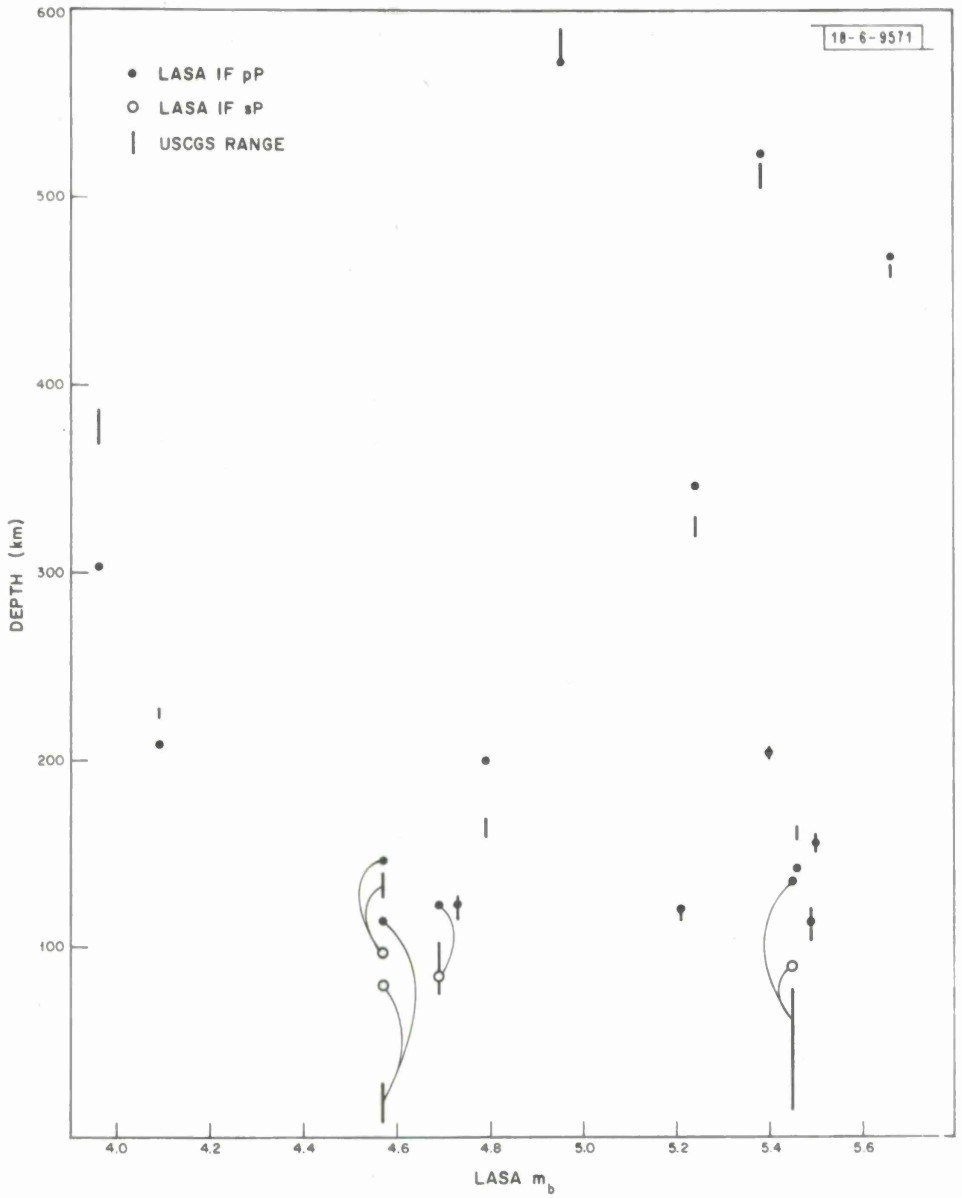

(b) Deep events.

Fig. 25. Continued.

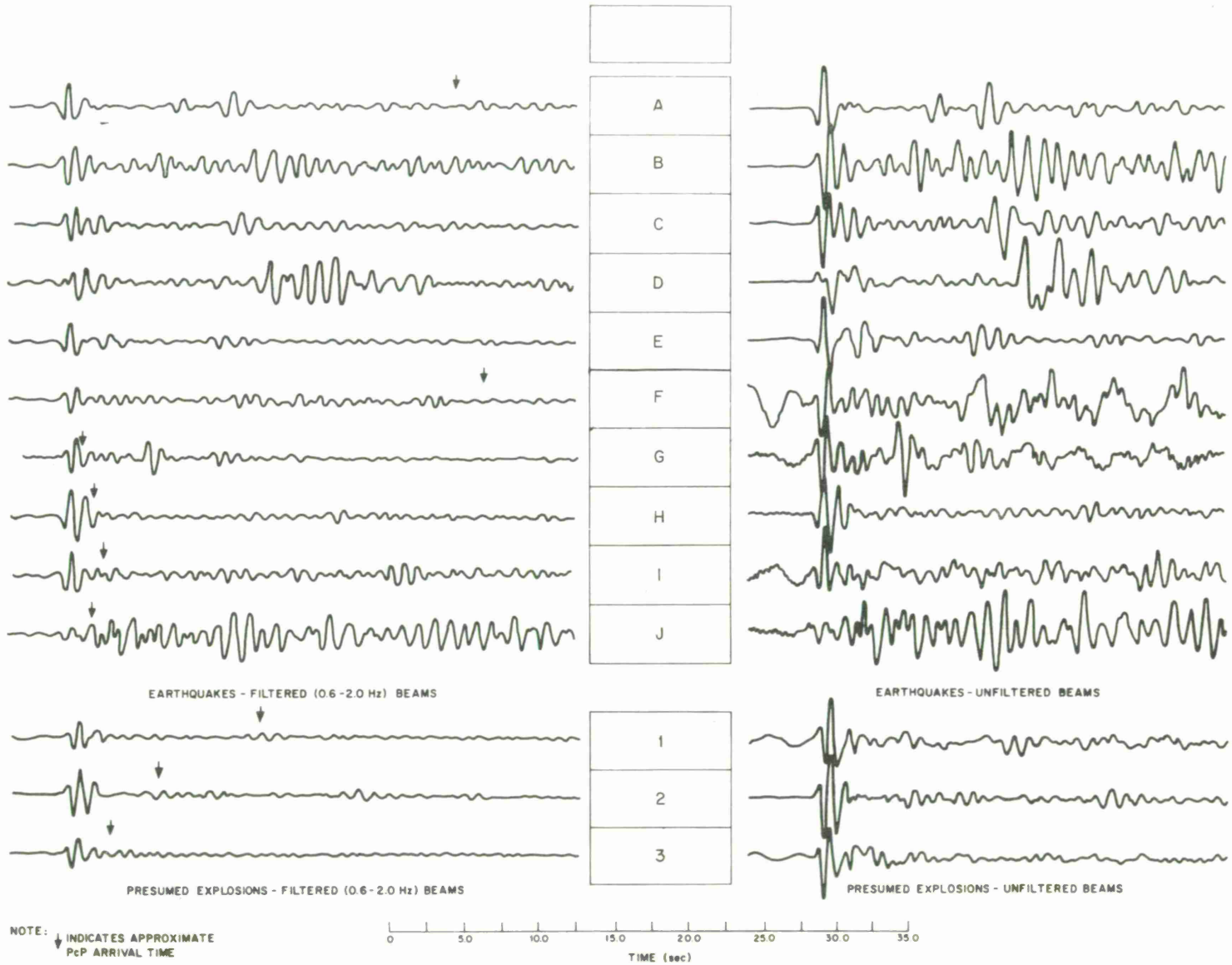

Fig. 26. Waveforms for the most ambiguous events according to the modified spectral ratio criterion.

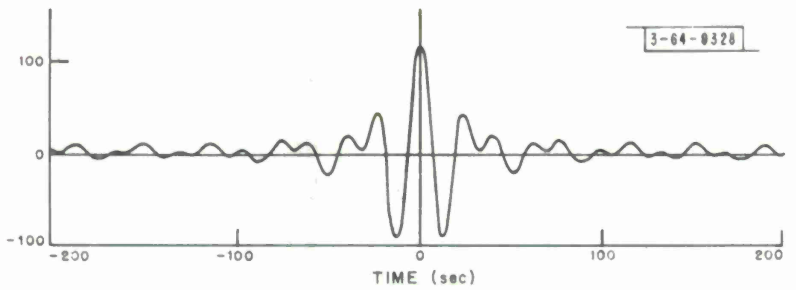

Fig. 27. Long period band-pass filter impulse response.

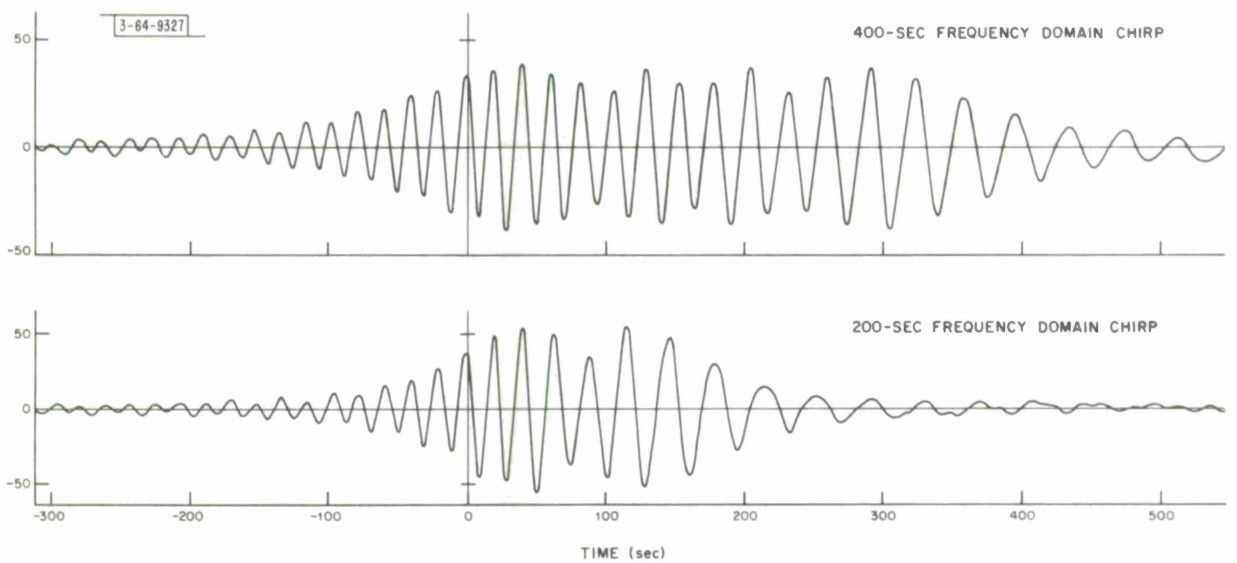

Fig. 28. Long period chirp filter impulse response.

DOCUMENT CONTROL DATA – R&D

(Security classification of title, body of abstract and indexing annotation must be entered when the overall report is classified)

1. ORIGINATING ACTIVITY *(Corporate author)* Lincoln Laboratory, M.I.T.	2a. REPORT SECURITY CLASSIFICATION Unclassified 2b. GROUP None

3. REPORT TITLE

A Large-Population LASA Discrimination Experiment

4. DESCRIPTIVE NOTES *(Type of report and inclusive dates)*

Technical Note

5. AUTHOR(S) *(Last name, first name, initial)*

Lacoss, Richard T.

6. REPORT DATE	7a. TOTAL NO. OF PAGES	7b. NO. OF REFS
8 April 1969	76	13

8a. CONTRACT OR GRANT NO. AF 19(628)-5167 b. PROJECT NO. ARPA Order 512 c. d.	9a. ORIGINATOR'S REPORT NUMBER(S) Technical Note 1969-24 9b. OTHER REPORT NO(S) *(Any other numbers that may be assigned this report)* ESD-TR-69-69

10. AVAILABILITY/LIMITATION NOTICES

This document has been approved for public release and sale; its distribution is unlimited.

11. SUPPLEMENTARY NOTES	12. SPONSORING MILITARY ACTIVITY
None	Advanced Research Projects Agency, Department of Defense

13. ABSTRACT

A computer program has been written and has been applied to LASA time series data from nearly 200 events in order to obtain data for discrimination studies. In general, the previously estimated performance of $M_S - m$, spectral ratio, and complexity have been corroborated. Some of the specific results are the following. Except for one anomalous earthquake, all shallow earthquakes with $m_b > 4.8$ and explosions with $m_b > 5.1$ have been correctly identified using $M_S - m_b$. No events with $m_b < 5.1$ could be unequivocally identified as explosions. However, the probability that an earthquake would be identified as such decreased to zero only gradually as m_b was reduced to about 4.0. A modification of spectral ratio has been made which introduced the option to make no decision concerning the nature of an event when the signal-to-noise ratio is not sufficiently large. The probability that no decision will be made is zero for $m_b > 4.8$ and unity for $m_b < 4.0$. The probability of correct identification is high for events which pass the signal-to-noise ratio tests. The period of short period P-waves may be a valuable discriminant at low magnitudes. Many earthquakes with magnitudes below 4.5 can be identified as such using the period data. Depth phase picks have been made for about 60 percent of the earthquakes in our population. About 70 to 95 percent of these picks correspond to valid depth phases. Unfortunately, depth phases were also picked for three presumed explosions.

14. KEY WORDS

LASA
seismic array
seismic discrimination
earthquakes
earth sensors